basilar impression might be a frequently found symptom of NS. Although the relationship between the positions of the cervical vertebrae and the hyoid bone has not been reported in TS, it has been investigated in healthy subjects (Moore and Dalley, 1999; Standring, 2008). We found that in the control group using the horizontal line, C3 was significantly superior to the hyoid bone, whereas C4 was significantly inferior to the hyoid bone. In a previous study using CT images and the FH plane as a reference, the centre of the body of the hyoid bone was most often at the level of C4, despite the hyoid bone being consistently described in contemporary anatomy textbooks as being level with C3 (Mirjalili *et al.*, 2012). The authors postulated that this disparity might relate to the use, by anatomy textbooks, of both the body and greater horn of the hyoid bone to describe its vertebral level, whereas they measured only from the centre of the body of the hyoid bone. The authors also pointed out that the vertebral level of the body of the hyoid bone seen in tracings of the lateral cervical radiograph varies depending on which reference plane is used (Figure 6). We measured the orientation of a horizontal reference line and FH plane in the control group according to Madsen's method (Madsen *et al.*, 2008) and confirmed that the average orientation was -3.28 ± 4.01 degrees similar to that reported in Madsen *et al* (-4.82 ± 4.63 degrees in that study). In agreement with the Mirjalili study, there was no difference in the statistical results when the FH plane was used instead (data not shown) or in the centres of both the hyoid bone and C4 as references, the reference point H in eight control subjects was located approximately level with the fourth cervical vertebra (data not shown). However, because in the present study we used alternative reference points for C3 and C4 (i.e. their most antero-inferior points) and the hyoid bone (i.e. its most antero-superior point) (Figure 6), the reference point of H was located significantly superior to the reference point in C4, despite the anatomy being demonstrably normal and in agreement with previous studies. We believe that this accounts for any discrepancy between our data and previous studies.

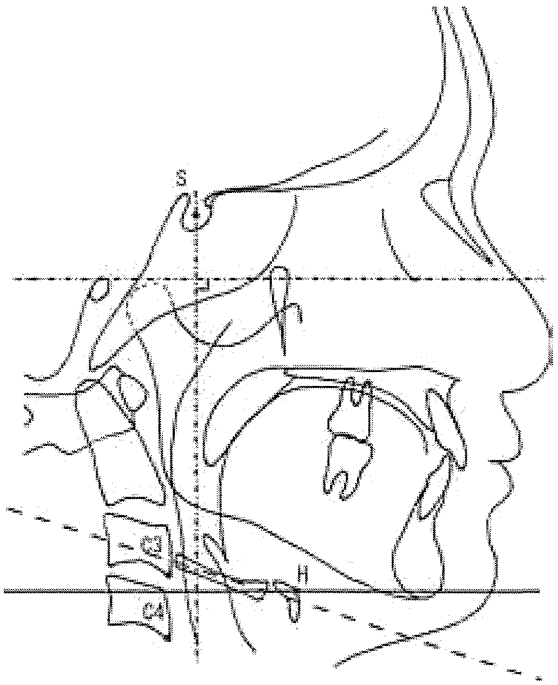

Figure 6 The vertebral level of structures in the neck depends in part on the choice of the reference plane. The solid line parallel to the Frankfort horizontal (FH) plane is not identical to the dashed line based on the inclination of the hyoid bone. The dashed-dotted lines show the FH plane and the reference line perpendicular to this originating in the sella turcica. Abbreviations: S, Sella; C3, the most antero-inferior point of the third cervical vertebra; C4, the most antero-inferior point of the fourth cervical vertebra; H, the most antero-superior point of the hyoid bone.

In this study, the number of subjects was small. However, it is difficult to recruit sufficient numbers of NS and TS subjects because they are rare syndromes. Further studies should investigate the results found here in a larger number of NS subjects. However, most previous studies listing cervical spine malformations commonly found in a variety of syndromes (Vastardis and Evans, 1996; Soni *et al.*, 2008) did not include NS in their analysis, depriving clinicians of an easy reference for recognizing and diagnosing NS in relation to other conditions affecting the cervical vertebrae. Our findings may help orthodontists recognize NS through the detection of basilar impression, a frequently found symptom of this syndrome, using cephalograms when patients attend orthodontic clinics for correction of malocclusion.

Conclusion

In the current study, we found that the odontoid tip extended significantly further past McGregor's line in the NS group compared with the TS and control groups, and that the positions of the third and the fourth cervical vertebrae in the NS group were significantly superior to those in the TS and control groups. Together, these data support a conclusion that basilar impression may be found frequently as a characteristic feature of NS.

Funding

Grants-in-Aid for Scientific Research Projects from the Japan Society for the Promotion of Science (#23792419); 'International Research Center for Molecular Science in Tooth and Bone Diseases', part of the Japanese Ministry of Education, Global Center of Excellence Program.

Acknowledgements

The authors would like to thank Assistant Professor Michiko Tsuji (Department of Maxillofacial Orthognathics,

Graduate School, Tokyo Medical and Dental University) for technical advice. We are indebted to Dr Keichi Kataoka, Dr Tomoko Ueno, and Dr Issareeya Ekprachayakoon for their help with data analysis, and we also gratefully acknowledge all other members of the Department of Maxillofacial Orthognathics, Graduate School, Tokyo Medical and Dental University for their support.

References

Asokan S, Muthu M S, Rathna Prabhu V 2007 Noonan syndrome: a case report. Journal of the Indian Society of Pedodontics and Preventive Dentistry 25: 144–147

Burrows E H 1981 Clinical relevance of radiological abnormalities of the craniovertebral junction. The British Journal of Radiology 54: 195–202

Chan A O *et al.* 2007 Prevalence of colorectal neoplasm among patients with newly diagnosed coronary artery disease.Journal of the American Medical Association 298: 1412–1419

Collins E, Turner G 1973 The Noonan syndrome–a review of the clinical and genetic features of 27 cases. The Journal of Pediatrics 83: 941–950

Dahlberg G 1940 Statistical Methods for Medical and Biological Students. George Allen & Unwin Ltd, London.

Delgado-López P D, Martín-Velasco V, Galacho-Harriero A M, Castilla-Díez J M, Rodríguez-Salazar A, Echevarría-Iturbe C 2007 Large chondroma of the dural convexity in a patient with Noonan's syndrome. Case report and review of the literature. Neurocirugía (Asturias, Spain) 18: 241–246

Emral M E, Akcam M O 2009 Noonan syndrome: a case report. Journal of Oral Science 51: 301–306

Ferrero G B *et al.* 2008 Clinical and molecular characterization of 40 patients with Noonan syndrome. European Journal of Medical Genetics 51: 566–572

Gabrielli O *et al.* 1990 Magnetic resonance imaging in the malformative syndromes with mental retardation. Pediatric Radiology 21: 16–19

Galarza M, Martínez-Lage J F, Ham S, Sood S 2010 Cerebral anomalies and Chiari type 1 malformation. Pediatric Neurosurgery 46: 442–449

Gardner D G, Shoback D M, Greenspan F S 2007 Greenspan's Basic & Clinical Endocrinology. 8th edition. McGraw Hill Medical, New York.

Goel A, Bhatjiwale M, Desai K 1998 Basilar invagination: a study based on 190 surgically treated patients. Journal of Neurosurgery 88: 962–968

Goel A, Shah A 2009 Reversal of longstanding musculoskeletal changes in basilar invagination after surgical decompression and stabilization. Journal of Neurosurgery Spine 10: 220–227

Guebert G M, Rowe L J, Yochum T R, Thompson J R, Masia C J 2005 Congenital anomalies and normal skeletal variants. In: Yochum T R, Rowe L J (eds.). Essentials of Skeletal Radiology. 3rd ed. Lippincott Williams & Wilkins, Philadelphia, pp. 257–403.

Hiyama S, Ono T, Ishiwata Y, Kuroda T 2001 Changes in mandibular position and upper airway dimension by wearing cervical headgear during sleep. American Journal of Orthodontics and Dentofacial Orthopedics 120: 160–168

Holder-Espinasse M, Winter R M 2003 Type 1 Arnold-Chiari malformation and Noonan syndrome. A new diagnostic feature? Clinical Dysmorphology 12: 275

Horowitz S L, Morishima A 1974 Palatal abnormalities in the syndrome of gonadal dysgenesis and its variants and in Noonan's syndrome. Oral Surgery, Oral Medicine, and Oral Pathology 38: 839–844

Ierardo G, Luzzi V, Panetta F, Sfasciotti G L, Polimeni A 2010 Noonan syndrome: A case report. European Journal of Paediatric Dentistry 11: 97–100

Kollias I, Krogstad O 1999 Adult craniocervical and pharyngeal changes–a longitudinal cephalometric study between 22 and 42 years of age. Part I: Morphological craniocervical and hyoid bone changes. European Journal of Orthodontics 21: 333–344

Kovero O, Pynnönen S, Kuurila-Svahn K, Kaitila I, Waltimo-Sirén J 2006 Skull base abnormalities in osteogenesis imperfecta: a cephalometric evaluation of 54 patients and 108 control volunteers. Journal of Neurosurgery 105: 361–370

Madsen D P, Sampson W J, Townsend G C 2008 Craniofacial reference plane variation and natural head position. European Journal of Orthodontics 30: 532–540

McGregor M 1948 The significance of certain measurements of the skull in the diagnosis of basilar impression. British Journal of Radiology 21: 171–181

Mirjalili S A, McFadden S L, Buckenham T, Stringer M D 2012 Vertebral levels of key landmarks in the neck. Clinical Anatomy 25: 851–857

Miyoshi Y, Yasuhara T, Date I 2011 Noonan syndrome with occipito-atlantal dislocation and upper cervical cord compression due to C1 dysplasia and basilar invagination. Neurologia Medico-chirurgica 51: 463–466

Moore K L, Dalley A F 1999 Clinically Oriented Anatomy, 4th Edition. Lippincott Williams & Wilkins, Philadelphia.

Peiris A, Ball M J 1982 Chiari (type 1) malformation and syringomyelia in a patient with Noonan's syndrome. Journal of Neurology, Neurosurgery, and Psychiatry 45: 753–754

Ricketts R M 1989 Provocations and Perceptions in Cranio-facial Orthopedics - Dental Science and Facial Art. Rocky Mountain Inc., Denver, pp. 797–803

Shaw A C, Kalidas K, Crosby A H, Jeffery S, Patton M A 2007 The natural history of Noonan syndrome: a long-term follow-up study. Archives of Disease in Childhood 92: 128–132

Sillence D O 1994 Craniocervical abnormalities in osteogenesis imperfecta: genetic and molecular correlation. Pediatric Radiology 24: 427–430

Soni P, Sharma V, Sengupta J 2008 Cervical vertebrae anomalies-incidental findings on lateral cephalograms. The Angle Orthodontist 78: 176–180

Standring S 2008 Gray's Anatomy: The Anatomical Basis of Clinical Practice, 40th edition. Edinburgh, Churchill Livingstone, pp. 405

Turner A M 2011 Noonan syndrome. Journal of Paediatrics and Child Health. Published online 19 July 2011, doi: 10.1111/j.1440-1754.2010.01970.x

van der Burgt I 2007 Noonan syndrome. Orphanet Journal of Rare Diseases 2: 4

van Der Burgt I, Brunner H 2000 Genetic heterogeneity in Noonan syndrome: evidence for an autosomal recessive form. American Journal of Medical Genetics 94: 46–51

Vastardis H, Evans C A 1996 Evaluation of cervical spine abnormalities on cephalometric radiographs. American Journal of Orthodontics and Dentofacial Orthopedics 109: 581–588

Yochum T R, Lindsay R 2005 Measurements in skeletal radiology. In: Yochum T R, Rowe L J (eds.) Essentials of Skeletal Radiology. 3rd edn. Lippincott Williams & Wilkins, Philadelphia, pp.197–256

CASE REPORT

Surgical Treatment for Scoliosis in Patients With Shprintzen-Goldberg Syndrome

Kota Watanabe, MD,† Eijiro Okada, MD,† Kenjiro Kosaki, MD,‡ Takashi Tsuji, MD,† Ken Ishii, MD,† Masaya Nakamura, MD,† Kazuhiro Chiba, MD,† Yoshiaki Toyama, MD,† and Morio Matsumoto, MD†*

Background: Shprintzen-Goldberg syndrome (SGS) is characterized by craniosynostosis and marfanoid habitus. The clinical findings of SGS include neurological, cardiovascular, connective tissue, and skeletal abnormalities. Among these skeletal findings, developmental scoliosis is recognized in half of all patients with SGS. However, no earlier reports have described the surgical treatment of scoliosis associated with SGS.

Methods: Four patients (2 boys and 2 girls; mean age at the time of surgery, 7.3 ± 4.4 y) with SGS who underwent surgical treatment for progressive scoliosis were reviewed. The radiologic findings, operative findings, and perioperative complications were evaluated.

Results: The mean preoperative Cobb angle was 102.8 ± 16.9 degrees. The curve patterns were a double curve in 2 cases and a triple curve in 2 cases. Local kyphosis at the thoracolumbar area was recognized in all the cases with a mean kyphosis angle of 49 ± 16 degrees. Growing rod procedures were performed in 2 patients, and posterior correction and fusion were performed in 2 patients. The mean correction rate was 45% in the patients who underwent the growing rod procedures at the time of growing rod placement and 51% in the patients who underwent posterior correction and fusion. Dislodgement of the proximal anchors occurred in 3 of the 4 patients. One patient developed pseudoarthrosis. Two patients developed deep wound infections, and implant removal was necessary in 1 patient.

Conclusions: Surgical treatment for scoliosis in patients with SGS was associated with a high incidence of perioperative and postoperative complications including implant dislodgements and deep wound infections attributable to poor bone quality and a thin body habitus, which are characteristic clinical features of this syndrome. Careful preoperative surgical planning and postoperative care are critical for the surgical treatment of scoliosis associated with SGS, especially in infants requiring multiple surgeries.

From the Departments of *Advanced Therapy for Spine and Spinal Cord Disorders; †Orthopedic Surgery; and ‡Pediatrics, Keio University School of Medicine, Tokyo, Japan.

Supported by none.

No funding was received for this study from any of the following organizations: National Institutes of Health (NIH); Wellcome Trust; Howard Hughes Medical Institute (HHMI).

Reprints: Morio Matsumoto, MD, Department of Orthopedic Surgery, Keio University School of Medicine, 35 Shinanomachi, Shinjuku, Tokyo, #160-8582, Japan. E-mail: morio@sc.itc.keio.ac.jp.

Level of Evidence: Level IV.

Key Words: Shprintzen-Goldberg syndrome, scoliosis, surgical treatment

(*J Pediatr Orthop* 2011;31:186–193)

Shprintzen-Goldberg syndrome (SGS), which is characterized by craniosynostosis and marfanoid habitus, was first reported by Shprintzen and Goldberg[1] in 1982. To date, approximately 40 cases of SGS have been reported.[2–5] An abnormality in the *FBN1* gene, which is related to Marfan syndrome,[6] is regarded as 1 of susceptible genes for SGS,[7–9] although this remains to be clarified in further genetic studies.[7,10,11] The clinical features of SGS include neurological, cardiovascular, connective tissue, and skeletal abnormalities. The skeletal features of SGS, such as a tall stature, arachnodactyly, foot deformity, joint hypermobility, and developmental scoliosis are similar to those of Marfan syndrome. The characteristic features that distinguish SGS from Marfan syndrome are craniofacial anomalies such as hypertelorism, downward-slanting palpebral fissures, a high-arched palate, micrognathia, low-set and posteriorly rotated ears, dolichocephaly, and a high prominent forehead caused by craniosynostosis.[2–5] Among these skeletal findings, developmental scoliosis is recognized in 50% of all patients reported with SGS.[4] However, to the authors' knowledge, the surgical treatment of scoliosis in patients with SGS has not been reported to date. In this study, we report 4 patients with SGS who underwent surgical treatments for progressive scoliosis.

METHODS

Four patients (2 male and 2 female; mean age at time of surgery, 7.3 ± 4.4 y) who underwent surgical treatments for severe scoliosis were included in this study. The diagnoses of SGS were made by a pediatrician specializing in genetic diseases based on the combinations of specific, earlier reported clinical features.[2,3,5] In 1 of the 4 patients (patient 2), a missense mutation in the *FBN1* gene was identified using a polymerase chain reaction analysis. The patients were followed for 4.4 ± 1.5 years (range, 2.5 to 6 y) after their first surgeries. The medical charts and radiographs of all the patients were reviewed

retrospectively, and the preoperative treatment, preoperative clinical findings, radiographic findings, surgical treatment, and perioperative and postoperative complications were investigated.

RESULTS

The clinical findings, radiologic findings, clinical courses, and surgical outcomes of the patients are summarized in Tables 1, 2, and 3. In 3 of the 4 patients, trunk deformities were recognized soon after the child began to sit or stand (patients 1, 2, and 3). However, one patient (patient 2) did not visit a pediatrician until the age of 4 years, and another patient (patient 1) was not referred to an orthopaedic surgeon until the age of 3 years, at which time the deformity had deteriorated to an extremely severe condition. The parents of patient 3 refused any treatment for scoliosis, although the patient was seen by a plastic surgeon until the age of years. Thus, none of the patients received brace treatment before surgery, and the Cobb angles at the time of the first recognition of the deformities could not be evaluated. In the radiographic evaluations, a double major curve pattern and a triple major curve pattern were recognized in 2 patients each

TABLE 1. Clinical Findings of 4 Cases

	Case 1	Case 2	Case 3	Case 4
Sex	Female	Male	Female	Male
Weight at operation	12.4 kg	11.5 kg	33 kg	44 kg
Centile	− 1.4 SD	− 1.1 SD	− 0.1 SD	0.1 SD
Hight at operation	103 cm	98 cm	146 cm	164 cm
Centile	1.6 SD	1.5 SD	1.6 SD	1.9 SD
Craniofacial				
Dolichocephaly	+	+	+	+
Fine/sparse hair			+	
High/prominent forehead	+	+	+	+
Ocular proptosis	+	+	+	+
Hypertelorism	+	+	+	+
Downslanting palpebral fissures	+	+	+	+
Strabismus	+			+
High, narrow palatal arch		+		+
Dental malocclusion	+	+	+	+
Micrognathia		+	+	
Skeletal				
Arachnodactyly	+	+	+	+
Camptodactyly	+	+	+	
Foot deformity	+		+	+
Pectus carinatum			+	
Joint hypermobility	+	+	+	
Craniosynostosis	+	+	+	+
Scoliosis	+	+	+	+
Cardiovascular				
Aortic root dilation		+		+
Mireal prolapse		+		
Mitral regurgitation				+
Arterial septal defect	+			
Tricuspid regurgitation		+		
Neurological				
Mental retardation		+	+	+
Other				
Minimal subcutaneous fat	+	+	+	+
Skin hyperelasticity	+	+	+	+
Myopia ± astigmatism	+		+	

SD indicates standard deviation.

TABLE 2. Radiological Findings of 4 Cases

Case	Sex	Age at Recognition of Scoliosis	Age at Surgery*	Postoperative Observation	Curve Pattern	Sagittal Alignment	Cobb Angle of Major Curve (°)	Flexibility of Major Curves (%)*	Dural Ectasia†
1	F	6 mo	3 y 7 mo	4 y	Triple	Thoracolumbar kyphosis (57 degrees)	53 (T1-7) 103 (T7-L1)	Not known	+
2	M	10 mo	4 y 10 mo	5 y	Double	Thoracolumbar kyphosis (66 degrees)	79 (T4-11) 100 (T11-L4)	72 (T4-11) 50 (T11-L4)	+
3	F	10 mo	10 y	2 y	Double	Thoracolumbar kyphosis (44 degrees)	113 (T5-T11) 105 (T11-L4)	40 (T5-T11) 33 (T11-L4)	—
4	M	7 y	12 y	3 y	Triple	Thoracolumbar kyphosis (29 degrees)	64 (T1-7) 78 (T7-L1) 52 (L1-5)	25 (T1-7) 38 (T7-L1) 27 (L1-5)	+

*Measured on supine side-bending films.
†Evaluated on MRI images.
F indicates female; M, male; MRI, magnetic resonance imaging.

TABLE 3. Surgical Results of 4 Cases

Case	Sex	Age at Surgery*	Operative Method	Operative Time (Min)*	Estimated Blood Loss (g)*	Correction Rate of Main Thoracic Curve (%)†	Complication	Present Treatment
1	F	3y 7mo	Growing rod	235	80	67	Implant failure at cranial anchors after first rod elongation Fourth replacements of distal anchors performed Deep wound infection that was successfully treated Proximal junctional kyphosis of 74 degrees	Growing rod
2	M	4y 10mo	Growing rod	325	168	55	Intraoperative left facet hook dislodgement at T5 Deep wound infection after first rod elongation Distal anchor removal because of persistent infection Distal implants removal after revision of distal anchors because of recurrence of infection	Brace
3	F	10y	Posterior correction and fusion	300	660	59	Reduction of motor evoked potentials during the curve correction Pseudarthrosis at distal end (L3/4), which was treated by posterior intervertebral fusion at L3/4 and L4/5	Brace
4	M	12y	Posterior correction and fusion	298	1080	89	Intraoperative bilateral T1 transverse processes hook dislodgements with fracture Reduction of motor evoked potentials during the curve correction Revision surgery of replacing dislodged hooks with pedicle screws at cranial ends 6mo after initial surgery Respiratory insufficiency that required reintubation for 3d Distal junctional kyphosis of 13degrees at L4/5	No

*Initial surgery for growing rod placement in case 1 and 2.
†Correction rates were calculated as a percentage change from the preoperative measurements.
F indicates female; M, male.

(Table 2). The magnitudes of the preoperative main curves were severe, with a mean Cobb angle of 102.8 ± 16.9 degrees (range, 78 to 113 degrees). The mean flexibility of the main curve evaluated using supine side-bending films was 41 ± 16% (range, 25% to 72%). Kyphosis at the thoracolumbar area was recognized in all the patients, with a mean kyphosis angle of 49 ± 16 degrees (29 to 66 degrees). Dural ectasias were recognized in 3 patients. Surgical treatments using a growing rod system were performed in 2 patients (patients 1 and 2), and posterior correction and fusion surgeries were performed in 2 patients (patients 3 and 4) (Table 3). The mean correction rate of the main curve at the time of the initial surgery was 47 ± 15% (range, 44% to 51%). The thoracolumbar kyphosis corrections during the initial surgeries were satisfactory except in patient 3, who experienced a dislodgement of the cranial anchor during kyphosis correction. Cefazolin (20 to 40 mg/kg) was administrated intravenously as a prophylactic antibiotic in all the cases at 30 minutes before the start of the operation, 3 hours after incision, soon after the operation, and 12, 24, 36, or 48 hours after operation.

Regarding complications, intraoperative implant dislodgement occurred in 2 cases because of fractures of the facets and transverse process (patients 1 and 4). Postoperative implant dislodgement occurred in 2 patients (patients 2 and 4). One patient developed pseudoarthrosis at distal end of the fusion area (L3/4) with a correction loss of 14 degrees and a symptom of severe low back pain at 2 years after surgery (patient 3). She underwent revision surgery of posterior intervertebral fusion at L3/4 and L4/5. Deep wound infections occurred in 2 patients (patients 1 and 2), and eventually resulted in implant removal in 1 patient (patient 2). *Staphylococcus epidermidis* was isolated from patient 1, and Methicillin-susceptible *Staphylococcus aureus* was isolated from patient 2. Postoperative respiratory insufficiency requiring reintubation and ventilator

control for 3 days occurred in 1 patient (patient 4). Distal junctional kyphosis at L4/5 without any clinical symptoms was recognized in 1 case 4 years after the initial surgery (patient 4). An apparent increase in kyphosis from 10 degrees before surgery to 74 degrees at 6 years after surgery was recognized in the upper thoracic area (T1-T6) in 1 patient (patient 1).

Patient 1

A female patient was found to have scoliosis at the age of 6 months. Although she was followed by a pediatrician for an arterial septal defect, she was not referred to an orthopaedic surgeon until the age of 3 years, at which time her scoliosis had deteriorated to 80 degrees. She was referred to our department at the age of 3 years and 6 months; at presentation, she weighed 12.4 kg (− 1.4 SD) and was 103 cm tall (1.6 SD). X-ray films showed a triple major curve pattern with a Cobb angle of 53 degrees at T1-T7, 103 degrees at T7-L1, and 60 degrees at L1-5. The kyphosis angle at the thoracolumbar area (T9-L3) was 57 degrees. Surgical treatment using a growing rod system was begun at the age of 3 years and 7 months. Claw hooks were placed at T2 and T3 as proximal anchors, and pedicle screws were placed at L3 and L4 as distal anchors. Four months after the surgery, soon after the first rod lengthening, the bilateral proximal anchors were dislodged as a result of fractures of the transverse processes. Despite repeated proximal anchor replacements, the hooks dislodged 3 times and the pedicle screws dislodged once. Finally, the patient is treated by growing rod system with hooks at 3 levels of T1-3 as proximal anchors. However, the proximal thoracic kyphosis (T1-7) gradually increased to 74 degrees at 5 years after surgery. Thus, a brace treatment that regulated neck flexion was applied to prevent the progression of proximal thoracic kyphosis beginning 3 years after the first operation. The patient also suffered a deep wound infection at the proximal anchor site, which healed successfully after debridement and irrigation at 3 years and 6 months after surgery. *S. epidermidis* was isolated from the wound.

Patient 2

A male patient was observed by his mother to have a trunk deformity when he first stood up at the age of 10 months. However, he did not visit a pediatrician to receive treatment for his deteriorating trunk deformity until the age of 4 years and 1 month. He was diagnosed as having SGS and was referred to our department at the age of 4 years and 3 months for the treatment of his spinal deformity. His weight was 11.5 kg (− 1.1 SD) and his height was 98 cm (1.5 SD). He presented with the characteristic features of SGS, listed in Table 1 (Fig. 1). A missense mutation in the *FBN1* gene was identified using a polymerase chain reaction analysis. X-ray films showed a double major curve pattern with a Cobb angle of 79 degrees at T4-T11 and 100 degrees at T11-L4 (Fig. 2A). A kyphosis of 66 degrees was recognized at the thoracolumbar area (T11-L3) (Fig. 2B). Surgical treatment using a growing rod system was started at the age of 4 years and 10 months. During the first surgery, claw hooks were placed at T4 and

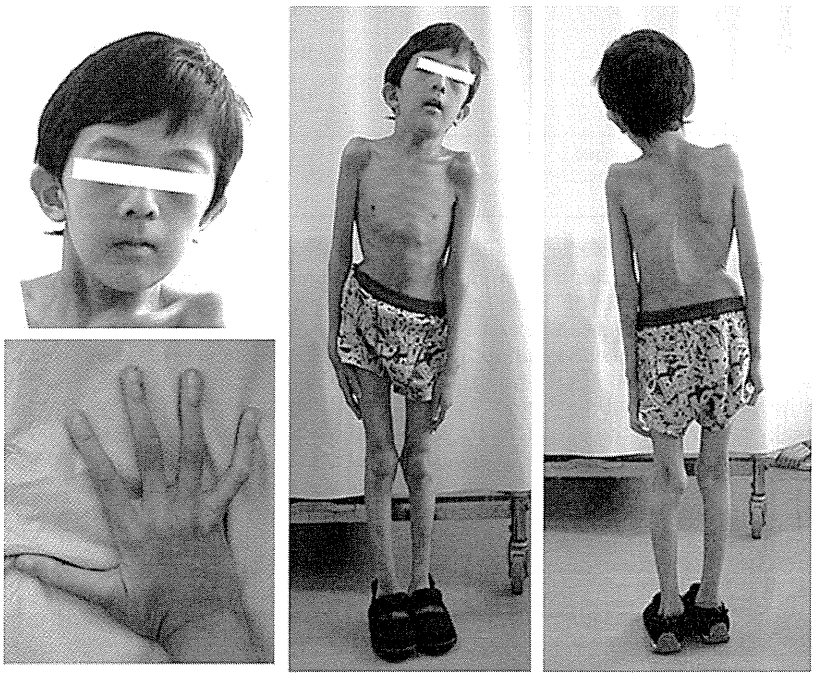

FIGURE 1. Clinical features of patient 2. The patient was a 4-year-old boy with a weight of 12.4 kg (− 1.1 SD) and a height of 103 cm (1.5 SD).

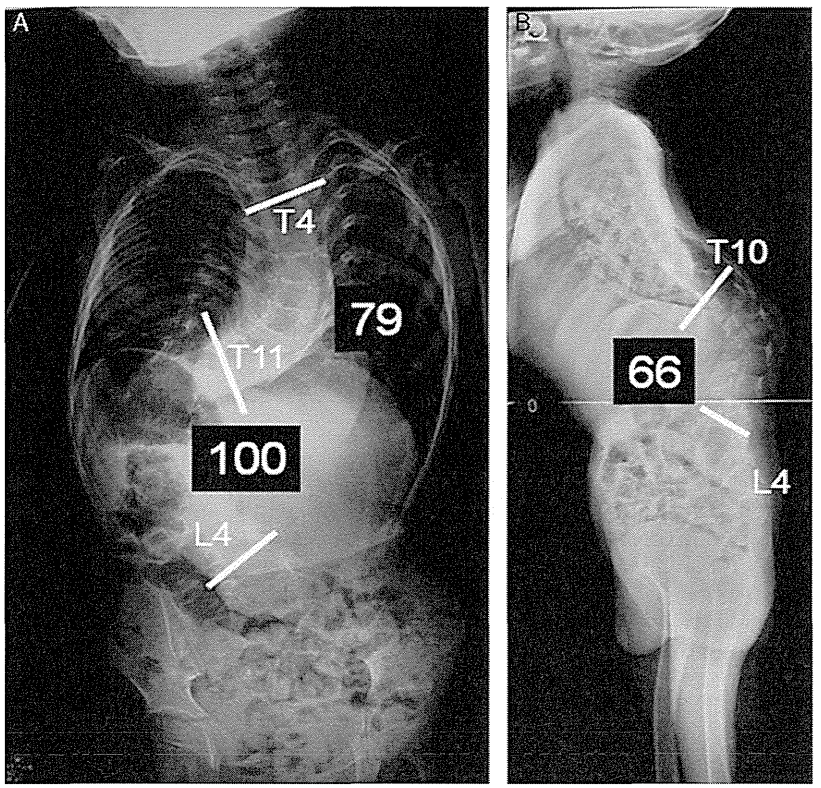

FIGURE 2. Preoperative radiographs of Patient 2. A double curve pattern with Cobb angles of 79 and 100 degrees (A) and local kyphosis of 66 degrees at the thoracolumbar junction are shown (B).

T5 as the proximal anchors and pedicle screws were placed only at L4 as distal anchors, as the patient was too thin to accommodate multiple screws. However, the hooks at T5 dislodged with fractures of the facets, possibly because of the poor bone quality, at the time of kyphosis correction using the cantilever technique. Postoperatively, the curves were corrected to 49 degrees at T4-T11 and 57 degrees at T11-L4, with correction rates of 38% and 45%, respectively (Fig. 3A). The kyphosis at the thoracolumbar area was corrected to 42 degrees (Fig. 3B). Five months after the surgery, the discharge of pus was recognized from a skin sore in the lumbar area just above the pedicle screws. As the infection did not subside after 2 surgical debridements, the distal anchors were removed at 9 months after the first surgery. Six months after their removal, growing rod treatment was restarted by placing distal anchors at L5. However, the deep wound infection recurred, and the implants were finally removed at 22 months after the first operation. At present, 6 years after the first surgery, the patient is being treated with a brace, and the Cobb angle of the main curve is 87 degrees (Fig. 3C) with a kyphosis of 125 degrees (Fig. 3D).

Patient 3

A female patient was found to have scoliosis at the age of 10 months. Although her scoliosis was pointed out by a plastic surgeon, her parents refused brace or surgical treatment for her. At the age of 11 years and 2 months, she was referred to our department for severe spinal deformity. She presented with the characteristic features of SGS, as listed in Table 1 (Fig. 4). X-ray films showed a double major curve pattern with a Cobb angle of 113 degrees at T5-T11 and 105 degrees at T11-L4 (Fig. 5A). A kyphosis of 44 degrees was recognized at the thoracolumbar area (T10-L3) (Fig. 5B). The Risser sign was 0, and the triradiate cartilages were closed. Posterior correction and fusion surgery were performed at the age of 11 years and 4 months. As her bone quality was poor, many segmental pedicle screws as possible were used to avoid implant dislodgement. Although an adequate number of pedicle screws were placed, the dislodgement of a few pedicle screws was observed on the concave side during curve correction. Moreover, a reduction in the motor-evoked potentials, which was restored after reversing the correction, was recognized during the curve correction. Thus, the endeavor to obtain a maximum correction was abandoned, and the main curves were corrected to Cobb angles of 50 and 52 degrees, respectively (Fig. 5C). The kyphosis at the thoracolumbar junction was corrected to 6 degrees (Fig. 5D). At 2 years after surgery, she developed pseudarthrosis at distal end of the fusion area (L3/4) with a correction loss of 14 degrees and a symptom of severe low back pain. She

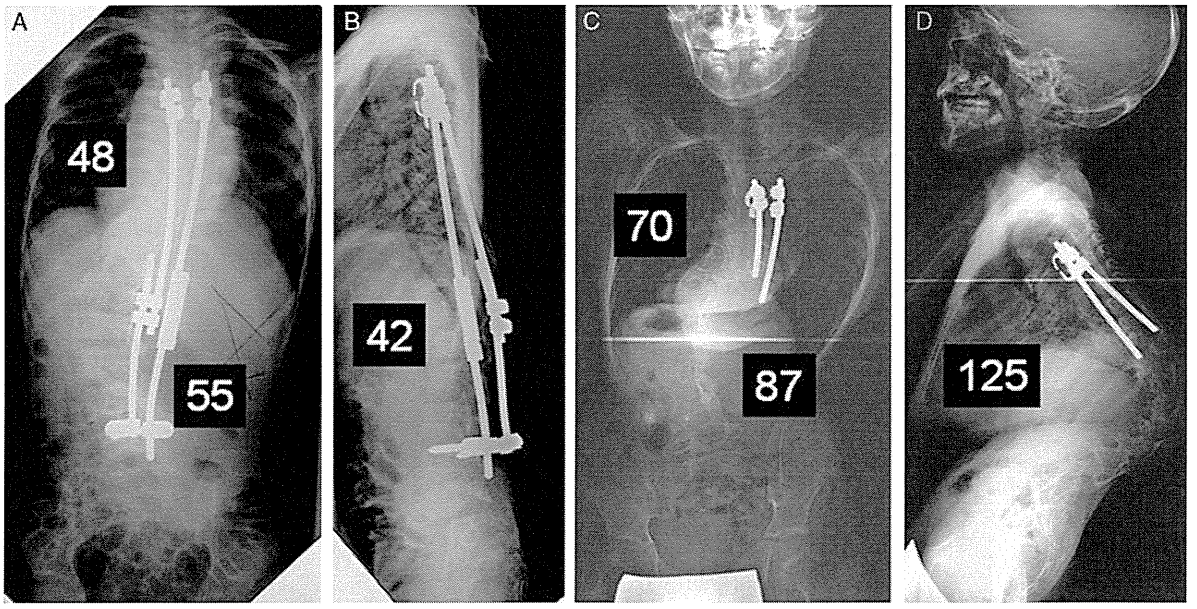

FIGURE 3. Postoperative radiographs of Patient 2. Growing rod treatment was started at the age of 4 years and 10 months (A, B). Postoperatively, the curves were corrected to 49 and 57 degrees (A). Kyphosis at the thoracolumbar area was corrected to 42 degrees (B). The distal anchors were finally removed due to deep wound infection at 22 months after the first operation. At present, 5 years after the first surgery, the Cobb angle of the main curve is 87 degrees (C) and the kyphosis is 125 degrees (D).

underwent revision surgery of posterior intervertebral fusion at L3/4 and L4/5. She was applied bed rest for 4 weeks and then trunk cast for 6 weeks after surgery.

Patient 4

A male patient was referred to our hospital at the age of 12 years and 6 months with a weight of 44 kg (0.1 SD) and a height of 164 cm (1.9 SD). Although he had been followed by a pediatrician for a cardiovascular problem and scoliosis was pointed out at the age of 7 years, he was not referred to an orthopaedic surgeon until the age of 12 years and 3 months; thus, no brace treatment was performed preoperatively. X-ray films showed a triple major curve pattern with a Cobb angle of 64 degrees at T1-T7, 78 degrees at T7-L1, and 52 degrees at L1-L5. A kyphosis of 29 degrees was recognized in the thoracolumbar area (T9-L3). The Risser sign was 0, and the triradiate cartilages were closed. Posterior correction and fusion surgery were performed at the age of 12 years and 9 months. As his bone quality was

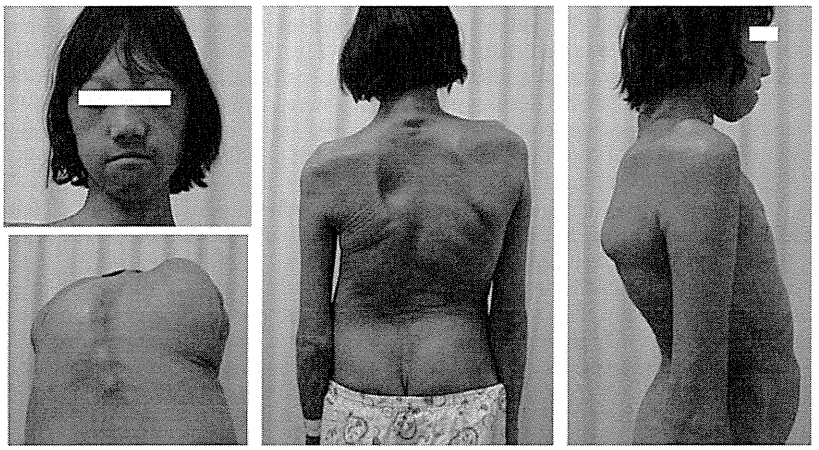

FIGURE 4. Clinical features of Patient 3. The patient was a 10-year-old girl with a weight of 33 kg (−0.1 SD) and a height of 146 cm (1.6 SD).

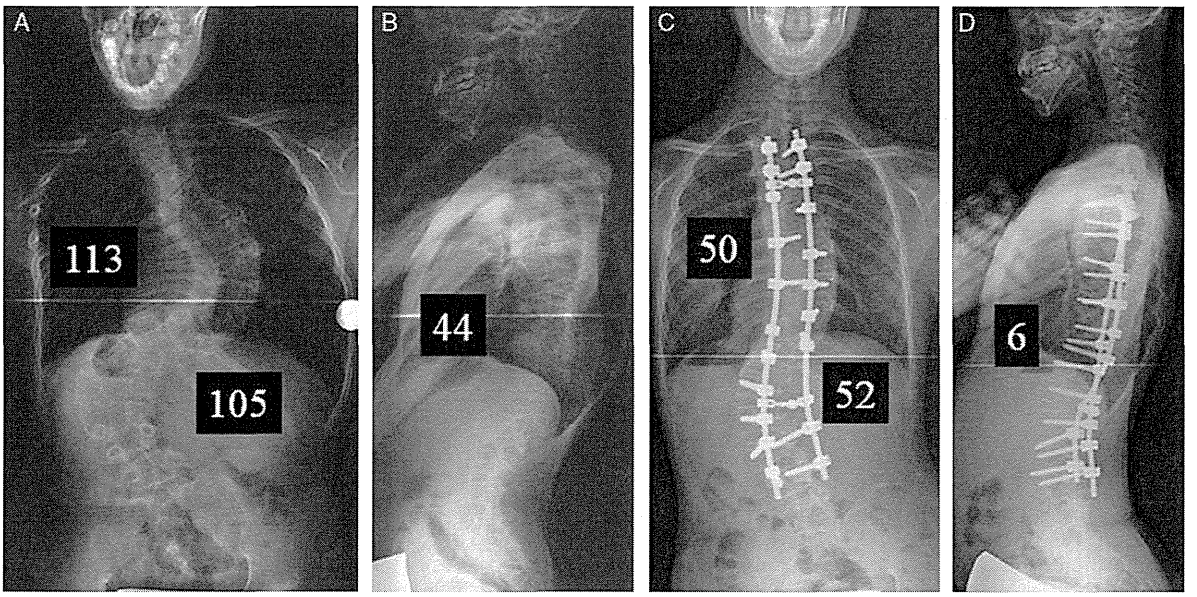

FIGURE 5. Radiographical findings of Patient 3. A double curve pattern with Cobb angles of 113 and 105 degrees (A) and local kyphosis of 44 degrees at the thoracolumbar junction are shown (B). Postoperatively, the main curves were corrected to Cobb angles of 50 and 52 degrees (C), and the kyphosis was corrected to 6 degrees (D).

poor, segmental anchors (screws, hooks) were placed at as many sites as possible to avoid implant dislodgement. However, the hooks at T1 were dislodged because of fractures of the transverse processes during curve correction. Ultrahigh molecular weight polyethylene fiber tapes (Alfresa Pharma, Osaka, Japan) were used to fix the rods to the T1 lamina, instead of using hooks. A reduction in motor-evoked potentials, which was restored after reversing the correction, was recognized during the curve correction. Postoperatively, the patient developed respiratory insufficiency requiring reintubation and assisted respiration for 3 days. Six months after the surgery, because of marked correction loss arising from the dislodgement of the proximal anchors, a revision surgery was performed and pedicle screws were placed at the right T1 and T2 and the left T2. Finally, the curves were corrected to 31degrees at T1-T7, 17 degrees at T7-L1, and 3 degrees at L1-L5. The thoracolumbar kyphosis was corrected to 42 degrees. The development of a junctional kyphosis of 13 degrees at L4/5, without any complaints, was recognized at 4 years after the first surgery.

DISCUSSIONS

The present series of patients with SGS indicated that the natural history of spinal deformity might start during infantile, and then finally would progress to very severe extent requiring surgical treatment. Unfortunately, none of the patients in this series had received brace treatment because the patients had been followed by doctors who might not have suspected the spinal deformities; thus, we could not know how effective brace treatment would be if brace treatment was applied within the extent of conservative treatment. However, as surgical treatment has a high risk of complications, we propose that thorough nonsurgical treatment including brace treatment or trunk cast be considered as alternative treatments to postpone surgical treatment as long as possible, especially in young kids as patient 1 or 2. If surgical treatments were not avoidable, preoperative evaluation by a pediatric cardiologist was compulsory as majority of the patient would accompany cardiac diseases. In addition, pulmonary function test including blood gas assessment should be performed suspecting restricted pulmonary dysfunctions or other malfunctions of respiratory system. The mean postoperative correction rate for the main curves (47%) was relatively low, compared with reported rates for severe scoliosis secondary to other diseases treated by pedicle screw construct.[12] One reason for this difference might be the poor bone quality, which prohibited large stresses on the anchors during correction. Another reason might be the rigidity of the curves in adolescents. The preoperative flexibilities were higher in the infants and much lower in the adolescents.

Intraoperative spinal cord monitoring of motor or sensory spinal evoked potentials should be performed during surgical treatment because the risk of injuring the spinal cord might be relatively high, as the correction of thoracolumbar kyphosis might increase the risk of neurological damage. In this study, reductions in motor-evoked potentials were recognized during curve corrections in 2 of the 4 cases. To prevent intraoperative neurological complications and/or to assess neurological

vulnerability preoperatively, halo gravity treatment[13] or extension over a bolster x-ray, may be a useful addition to the preoperative evaluations to determine the extent of the "safe" extension correction that can be achieved.

The surgical treatments for scoliosis in patients with SGS in our series were associated with a high complication rate. One such complication was implant dislodgement that was attributed to the extremely poor bone quality of the spine. In fact, hook or pedicle screw dislodgement was recognized during or after surgery in 3 of the 4 patients in this study. Such poor bone quality in patients with SGS might be related to an abnormality in fibrillin, which is considered to be associated with Marfan syndrome.[14,15] Kyphosis at the thoracolumbar area might also increase the risk of anchor dislodgement, as the correction of kyphosis places an excessive pull-out force on the anchors. Moreover, frequently observed dural ectasia associated with a narrowed pedicle and lamina can also increase the risk of anchor dislodgement. To prevent implant dislodgement, as many segmental anchors (screws, hooks, wires) as possible should be used. Hooks might be preferable to pedicle screws as proximal anchors when the pedicles are too narrow to accommodate pedicle screws. Additional sublaminar wiring or taping using ultrahigh molecular weight polyethylene fiber tapes should also be considered to reduce the risk of implant dislodgement. For growing rod treatment, anchor placements with abundant graft bone 3 to 4 months before curve correction with rod placement might be effective for patients with poor bone quality or severe kyphosis . Other techniques, such as preoperative halo gravity treatment,[13] anterior release, or intraoperative halo femoral traction,[16] which are often used for the surgical treatment of patients with severe deformities, should be considered. Postoperative brace application should also be considered to reduce the risk of implant dislodgement or pseudoarthrosis.

In our series, the 2 patients who were treated with growing rod systems developed deep wound infections after rod lengthening. The deep wound infections might have been associated with skin sores. All the 4 patients were skeletally very thin, with heights ranging from 1.5 to 1.9 SD for their ages and weights ranging from −1.4 to 0.1 SD. The prominence of implants caused by suboptimal implant coverage by the skin and subcutaneous tissues is a risk factor for wound infections, especially in patients treated with growing rod systems that require multiple surgeries. Thus, soft tissues should be handled with extreme care to prevent skin sores.

In conclusion, 4 patients with SGS who underwent surgical treatment for severe scoliosis are reported. Surgical treatment was associated with a high incidence of complications including implant failures and deep wound infections attributable to the poor bone quality and thin bodily habitus, which are characteristics of this syndrome.

REFERENCES

1. Shprintzen RJ, Goldberg RB. A recurrent pattern syndrome of craniosynostosis associated with arachnodactyly and abdominal hernias. *J Craniofac Genet Dev Biol.* 1982;2:65–74.
2. Ades LC, Morris LL, Power RG, et al. Distinct skeletal abnormalities in four girls with Shprintzen-Goldberg syndrome. *Am J Med Genet.* 1995;57:565–572.
3. Robinson PN, Neumann LM, Demuth S, et al. Shprintzen-Goldberg syndrome: fourteen new patients and a clinical analysis. *Am J Med Genet A.* 2005;135:251–262.
4. Greally MT, Carey JC, Milewicz DM, et al. Shprintzen-Goldberg syndrome: a clinical analysis. *Am J Med Genet.* 1998;76:202–212.
5. Saal HM, Bulas DI, Allen JF, et al. Patient with craniosynostosis and marfanoid phenotype (Shprintzen-Goldberg syndrome) and cloverleaf skull. *Am J Med Genet.* 1995;57:573–578.
6. Katzke S, Booms P, Tiecke F, et al. TGGE screening of the entire FBN1 coding sequence in 126 individuals with marfan syndrome and related fibrillinopathies. *Hum Mutat.* 2002;20:197–208.
7. Kosaki K, Takahashi D, Udaka T, et al. Molecular pathology of Shprintzen-Goldberg syndrome. *Am J Med Genet A.* 2006;140:104–108; author reply 109–110.
8. Hatchwell E. Shprintzen-Goldberg syndrome results from mutations in fibrillin-1, not monosomy 22q11. *J Pediatr.* 1997;131:164–165.
9. Sood S, Eldadah ZA, Krause WL, et al. Mutation in fibrillin-1 and the Marfanoid-craniosynostosis (Shprintzen-Goldberg) syndrome. *Nat Genet.* 1996;12:209–211.
10. Loeys BL, Chen J, Neptune ER, et al. A syndrome of altered cardiovascular, craniofacial, neurocognitive and skeletal development caused by mutations in TGFBR1 or TGFBR2. *Nat Genet.* 2005;37:275–281.
11. Watanabe Y, Yano S, Koga Y, et al. P1148A in fibrillin-1 is not a mutation leading to Shprintzen-Goldberg syndrome. *Hum Mutat.* 1997;10:326–327.
12. Watanabe K, Lenke LG, Bridwell KH, et al. Comparison of radiographic outcomes for the treatment of scoliotic curves greater than 100 degrees: wires versus hooks versus screws. *Spine.* 2008;33:1084–1092.
13. Rinella A, Lenke L, Whitaker C, et al. Perioperative halo-gravity traction in the treatment of severe scoliosis and kyphosis. *Spine.* 2005;30:475–482.
14. Carter N, Duncan E, Wordsworth P. Bone mineral density in adults with Marfan syndrome. *Rheumatology (Oxford).* 2000;39:307–309.
15. Moura B, Tubach F, Sulpice M, et al. Bone mineral density in Marfan syndrome: a large case-control study. *Joint Bone Spine.* 2006;73:733–735.
16. Qiu Y, Liu Z, Zhu F, et al. Comparison of effectiveness of Halo-femoral traction after anterior spinal release in severe idiopathic and congenital scoliosis: a retrospective study. *J Orthop Surg.* 2007;2:23.

our data provide proof of concept support for targeting this molecule and its multi-cellular functions in psoriatic skin. Targeting VEGF topically may provide an effective new approach for treating mild-to-moderate psoriasis skin lesions by inhibiting angiogenesis and reducing leukocyte infiltration and KC proliferation.

Funding support

NLW is supported in part by grants from the National Institutes of Health (P30AR39750, P50AR05508, RO1AR063437; RO1AR062546) and the National Psoriasis Foundation.

Acknowledgments

The authors apologize to colleagues whose work could not be cited because of the space constraints. We thank Dr. John Rudge (Regeneron Pharmaceuticals, Tarrytown, NY) for providing VEGF-Trap and Dr. Thomas McCormick for feedback on the manuscript.

References

[1] Yancopoulos GD, Davis S, Gale NW, Rudge JS, Wiegand SJ, Holash J. Vascular-specific growth factors and blood vessel formation. Nature 2000;407:242–8.
[2] Kunstfeld R, Hirakawa S, Hong YK, Schacht V, Lange-Asschenfeldt B, Velasco P, et al. Induction of cutaneous delayed-type hypersensitivity reactions in VEGF-A transgenic mice results in chronic skin inflammation associated with persistent lymphatic hyperplasia. Blood 2004;104:1048–57.
[3] Jung K, Lee D, Lim HS, Lee S-I, Kim YJ, Lee GM, et al. Double anti-angiogenic and anti-inflammatory protein valpha targeting VEGF-A and TNF-alpha in retinopathy and psoriasis. J Biol Chem 2011;286:14410–18.
[4] Xia YP, Li B, Hylton D, Detmar M, Yancopoulos GD, Rudge JS. Transgenic delivery of VEGF to mouse skin leads to an inflammatory condition resembling human psoriasis. Blood 2003;102:161–8.
[5] Akman A, Yilmaz E, Mutlu H, Ozdogan M. Complete remission of psoriasis following bevacizumab therapy for colon cancer. Clin Exp Dermatol 2009;34:e202–4.
[6] Fournier C, Tisman G. Sorafenib-associated remission of psoriasis in hypernephroma: case report. Dermatol Online J 2010;16(17.).
[7] Wolfram JA, Diaconu D, Hatala DA, Rastegar J, Knutsen DA, Lowther A, et al. Keratinocyte but not endothelial cell specific overexpression of Tie2 leads to the development of psoriasis. Am J Pathol 2009;174:1443–58.
[8] Ward NL, Loyd CM, Wolfram JA, Diaconu D, Michaels CM, McCormick TS. Depletion of antigen-presenting cells by clodronate liposomes reverses the psoriatic skin phenotype in KC-Tie2 mice. Brit J Dermatol 2011;164:750–8.
[9] Schonthaler HB, Huggenberger R, Wculek SK, Detmar M, Wagner EF. Systemic anti-VEGF treatment strongly reduces skin inflammation in a mouse model of psoriasis. Proc Natl Acad Sci USA 2009;21264–69.

Doina Diaconu[a], Yi Fritz[a], Sean M. Dawes[a], Candace M. Loyd[a], Nicole L. Ward[a, b, *]
[a]*Department of Dermatology, Case Western Reserve University, Cleveland, OH 44106, USA;*
[b]*The Murdough Family Center for Psoriasis, University Hospitals Case Medical Center, Cleveland, OH 44106, USA*

*Corresponding author at: Case Western Reserve University, Department of Dermatology BRB519, 10900 Euclid Avenue, Cleveland, OH 44106, USA.
Tel.: +1 216 368 1111; fax: +1 216 368 0212
E-mail address: Nicole.ward@case.edu (N. Ward)

19 April 2013

http://dx.doi.org/10.1016/j.jdermsci.2013.08.005

Letter to the Editor

Co-existence of mutations in the *FBN1* gene and the *ABCC6* gene in a patient with Marfan syndrome associated with pseudoxanthoma elasticum

To the Editor,

Marfan's syndrome (MFS) is a disease with an autosomal dominant mode of inheritance that is manifested by characteristic skeletal abnormalities, including arachnodactyly, cardiovascular lesions (such as aortic dilatation), and ocular manifestations (such as ectopia lentis) [1]. The *FBN1* gene [2], which encodes fibrillin-1 (a component of elastic fibers), has been identified as the responsible gene. Pseudoxanthoma elasticum (PXE) is an autosomal recessive disorder that causes the ectopic mineralization of elastic fibers in soft connective tissues and mainly affects the eyes, skin, and cardiovascular system. The precise pathomechanisms of elastic fiber degeneration in PXE have not been fully elucidated despite a number of extensive studies [3]. The disease is linked to mutations in the ATP-binding cassette sub-family C member 6 (*ABCC6*) gene [4,5]. Here, we report the case of a patient who exhibited the clinical manifestations of both MFS and PXE and in whom pathological gene mutations were detected in both the *FBN1* gene and the *ABCC6* gene.

In 2003, a 64-year-old, tall Japanese woman presented with skin eruptions in her nuchal area, axillae, and groin. She had previously experienced angina pectoris and had undergone bypass surgery for coronary stenosis. The patient's family history revealed that her mother had been tall and had died of heart disease when the patient was a small child. A history and physical examination of her father revealed that he had no noteworthy clinical findings. The patient was the 5th of 5 siblings, and the eldest sister and the 4th sister had both been tall. The eldest sister had suddenly died of unknown causes in early childhood, and the 4th sister had died of aortic dissection. The patient had two children, a 38-year-old son and a 36-year-old daughter, and both had skeletal abnormalities that included a tall stature and arachnodactyly. Her son had undergone a Bentall operation for aortic dissection and aortic valve regurgitation as a child. Dermatological and ophthalmological examinations revealed no evidence of PXE in either child. The patient's family tree is shown in Fig. 1A.

At the time of the patient's initial examination, she was 165 cm tall and had an arm span of 185 cm. Dolichocephaly, pectus carinatum, disproportionately long limbs for her height, and arachnodactyly were noted (Fig. 1B). Numerous papules ranging in color from normal to yellow arrayed in a cobblestone pattern were observed in the nuchal area, axillae, and groin (Fig. 1C). Ophthalmological examinations revealed angioid streaks on her retinas. Radiography revealed linear calcifications in the upper limbs. The pathological findings for skin biopsy specimens from the affected sites consisted of clumps of fragmented basophilic fibers in the middle and lower layers of the dermis (Fig. 1D). Granular deposits that stained positive with von Kossa stain (Fig. 1E) were observed in specimens from the same sites.

A genomic DNA analysis of the patient's blood revealed a monoallelic nonsense mutation (c. 5454C > A: exon 44, p.Cys1818Stop) in the *FBN1* gene (Fig. 2A). Exon sequencing of *ABCC6* was performed using primers designed to eliminate *ABCC6* pseudogenes for exons 1–9 [6] and those designed by Prime 3 for

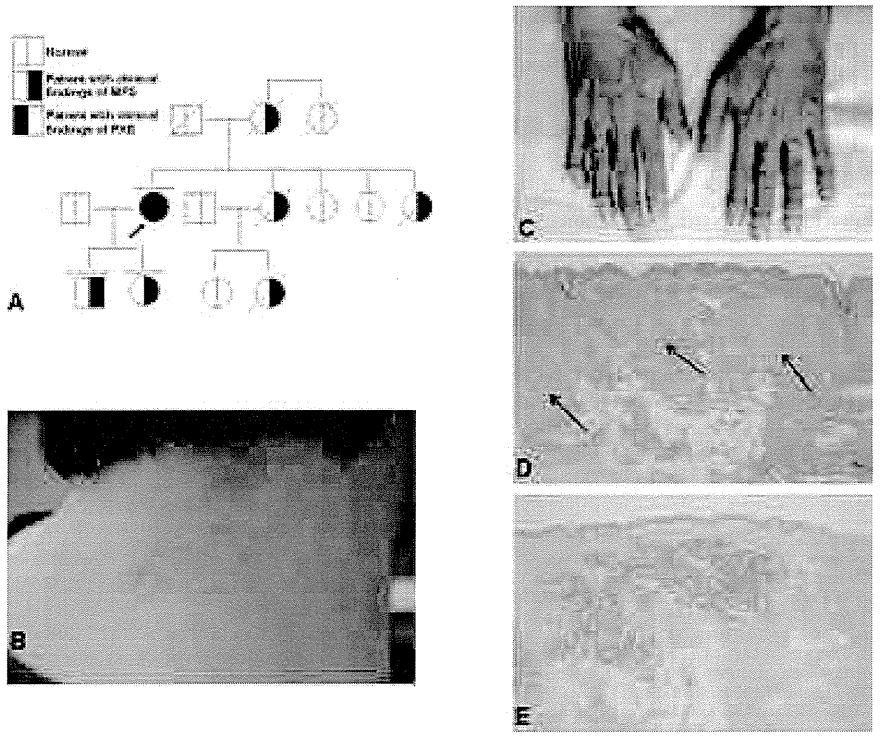

Fig. 1. Family tree, clinical findings, and pathological findings. (A) The patient's family tree. (B) Arachnodactyly. (C) Normal flesh color to yellow papules in a cobblestone pattern on the back of the patient's neck. (D) Clumps of fragmented basophilic fibers that look like thread waste are seen in the middle and lower layers of the dermis (hematoxylin and eosin, ×200). (E) Numerous granular deposits are seen among the clumps of fragmented fibers that have the appearance of thread waste (von Kossa stain, ×200).

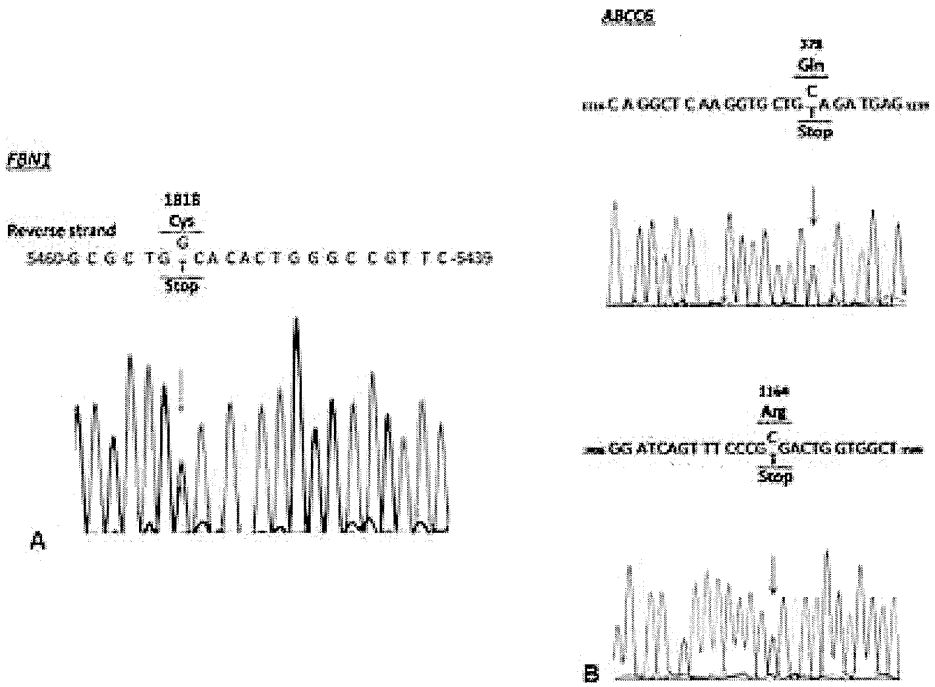

Fig. 2. Sequencing data of the patient's *FBN1* gene, which encodes fibrillin-1, and the *ABCC6* gene, which encodes ATP binding cassette C6 protein. (A) Sequence analysis of *FBN1*. A reverse sequence analysis of the portion of *FBN1* extending from c.5439 to c.5460 is shown. A monoallelic nonsense mutation (c.5454C > A, p.Cys1818Stop) was detected. (B) Sequence analysis of *ABCC6*. The results of sequence analyses of the portion of *ABCC6* extending from c.1116 to c.1139 and from 3486 to 3500 are shown. Compound heterozygous nonsense mutations (c.1132C > T, p.Gln378Stop and c.3490A > T, p.Arg1164Stop) were detected.

the other exons. The patient had two mutations in the ABCC6 gene: c.1132C > T in exon 9, p.Gln378Stop; and c.3490A > T in exon 24, p.Arg1164Stop (Fig. 2B). The patient's son had only the former mutation. Therefore, this patient had compound heterozygous nonsense mutations of *ABCC6*.

There has been one other report of a case of MFS and PXE in the same patient besides our own. The case was reported by Hidano et al. [7], similar to the present case, the previously reported patient was a member of a Japanese pedigree that exhibited the skeletal abnormalities associated with MFS, and the patient developed manifestations of both MFS and PXE. However, no search for gene mutations was performed in their case. Ours is the first report ever to describe MFS and PXE occurring in the same patient in whom mutations were confirmed in both the *ABCC6* gene and the *FBN1* gene. The concomitant presence of MFS and PXE seems to have been coincidental, but both conditions are hereditary diseases that give rise to elastic fiber abnormalities and to abnormalities in the same organs, including the cardiac blood vessels, and eyes. We plan to monitor the course of the presently reported patient to determine how her outcome compares with the outcome of patients who have only one of these diseases, either MFS or PXE.

References

[1] Burrows, Lovell CR. In: Tony B, Stephen B, Neil C, Christopher G, editors. Rook's textbook of dermatology. 7th ed., Oxford: Blackwell Science; 2004. p. 4621–31.
[2] Dietz HC, Cutting GR, Pyeritz RE, Maslen CL, Sakai LY, Corson GM, et al. Marfan syndrome caused by a recurrent de novo missense mutation in the fibrillin gene. Nature 1991;352:337–9.
[3] Uitto J, Li Q, Jiang Q. Pseudoxanthoma elasticum: molecular genetics and putative pathomechanisms. J Invest Dermatol 2010;130:661–70.
[4] Bergen AA, Plomp AS, Schuurman EJ, Terry S, Breuning M, Dauwerse H, et al. Mutation in *ABCC6* cause pseudoxanthoma elasticum. Nat Genet 2000;25:228–31.
[5] Lebwohl M, Nelder K, Pope FM, De Paepe A, Christiano AM, Boyd CD, et al. Classification of pseudoxanthoma elasticum. Report of a consensus conference. J Am Acad Dermatol 1994;30:103–7.
[6] Pulkkinen L, Nakano A, Ringpfeil F, Uitto J. Identification of ABCC6 pseudogenes on human chromosome 16p: implications for mutation detection in pseudoxanthoma elasticum. Hum Genet 2001;109:356–65.
[7] Hidano A, Nakajima S, Shimizu T, Kimata Z. Pseudoxanthoma elasticum associated with Marfan syndrome. Ann Dermatol Venereol 1979;106:503–5.

Shujiro Hayashi[a], Atsushi Utani[b], Akira Iwanaga[b], Yosuke Yagi[b], Hiroko Morisaki[c], Takayuki Morisaki[c], Yoichiro Hamasaki[a], Atsushi Hatamochi[a,*]

[a]*Department of Dermatology, Dokkyo Medical University, School of Medicine, Mibu, Tochigi, Japan*;
[b]*Department of Dermatology, Graduate School of Biomedical Sciences Nagasaki University, Nagasaki-city, Nagasaki, Japan*;
[c]*Department of Bioscience and Genetics, National Cerebral and Cardiovascular Center Research Institute, Suita, Osaka, Japan*
*Corresponding author at: Department of Dermatology, Dokkyo Medical University, School of Medicine 880 Kitakobayashi, Mibu, Tochigi 321-0293, Japan.
Tel.: +81 282 87 2154;
fax: +81 282 86 3470
E-mail address: hatamo@dokkyomed.ac.jp (S. Hayashi)

22 April 2013

http://dx.doi.org/10.1016/j.jdermsci.2013.07.007

Letter to the Editor

Birth, life, and death of the MAGE3 hypothesis of alopecia areata pathobiology

Dear Editor,

In this distinguished journal, we routinely read discovery stories that have been ultimately crowned by success. Instead, here we would like to share our trials and tribulations along a less felicitous, yet very instructive and educational research journey that brought us close to what we hoped to be a clinically important advance in understanding the pathobiology of alopecia areata (AA), a tissue-specific, T cell-dependent autoimmune disease [1].

Most currently available evidence suggests that, upon interferon (IFN)-γ-induced collapse of the hair follicle's (HF's) physiological immune privilege (IP), as yet unidentified follicular autoantigens are exposed to preexisting autoreactive $CD8^+$ T cells by ectopically expressed major histocompatibility (MHC) class I molecules within the epithelium of anagen hair bulbs [1,2]. Peptides derived from melanogenesis-associated autoantigens expressed only by melanin-producing anagen HFs are persuasive candidates as key autoantigens in AA [3]. Therefore, focusing on well-investigated MHC class I-restricted melanocyte-related antigens known to be recognized by $CD8^+$ T cells is a sensible AA research strategy (supplementary text S1).

Supplementary material related to this article can be found, in the online version, at http://dx.doi.org/10.1016/j.jdermsci.2013.07.014.

We thus hypothesized that it should be possible to detect cytotoxic $CD8^+$ T cells (CTLs) directed against MHC class-I restricted autoantigens (tyrosinase, MAGE-A2, and MAGE-A3 (MBL)), using pentamer technology [4] (Supplemental text S2). To test this hypothesis, peripheral blood mononuclear cells (PBMCs) were obtained from Japanese healthy controls and AA patients (Supplementary Table S1).

Initially, this approach yielded auspicious results: MAGE-A3-reactive $CD8^+$ T cells were found to be significantly increased in PBMCs in the acute phase of AA with multifocal lesions (AAM) and alopecia areata totalis (AAT) compared to healthy controls, chronic phase of AAM, or AAT/alopecia areata universalis (AU) (Fig. 1a and Fig. S1a and b and Supplementary text S3) ($p = 0.025$ by Kruskal–Wallis ANOVA). Furthermore, skin infiltrating T cells of an acute phase AA lesion from one patient, which were isolated as previously described [5], also showed an increased number of MAGE-A3 specific CTLs (Fig. 1b) as that in peripheral blood nuclear cells (PBMCs) from the same AA patients (Fig. 1c) compared to the average frequency of MAGE-$A3^+$ T cells in PBMCs from control subjects (Fig. 1a). This pilot finding suggested an enrichment of MAGE-$A3^+$ CTLs in lesional AA skin.

Supplementary material related to this article can be found, in the online version, at http://dx.doi.org/10.1016/j.jdermsci.2013.07.014.

Next, we probed whether such CTLs can produce IFN-γ after stimulation with MAGE-A3 (supplementary text S4). Indeed, IFN-γ protein expression was significantly increased in $CD8^+$ T cells from acute phase AA patients co-cultured with MAGE-A3 compared to healthy controls (Fig. 1d and supplementary Fig. S1c and d). Moreover, the percentage of MAGE-A3 specific CTLs

OPEN ACCESS Freely available online

PLOS | ONE

Prevalence of Dural Ectasia in Loeys-Dietz Syndrome: Comparison with Marfan Syndrome and Normal Controls

Atsushi K. Kono[1]*, Masahiro Higashi[2], Hiroko Morisaki[3], Takayuki Morisaki[3], Hiroaki Naito[2], Kazuro Sugimura[1]

1 Department of Radiology, Kobe University Graduate School of Medicine, Kobe Japan, **2** Department of Radiology, National Cardiovascular Research Center, Suita, Japan, **3** Department of Bioscience, National Cardiovascular Research Center, Suita, Japan

Abstract

Background and Purpose: Dural ectasia is well recognized in Marfan syndrome (MFS) as one of the major diagnostic criteria, but the exact prevalence of dural ectasia is still unknown in Loeys–Dietz syndrome (LDS), which is a recently discovered connective tissue disease. In this study, we evaluated the prevalence of dural ectasia in LDS according by using qualitative and quantitative methods and compared our findings with those for with MFS and normal controls.

Material and Methods: We retrospectively studied 10 LDS (6 males, 4 females, mean age 36.3 years) and 20 MFS cases (12 males, 8 females, mean age 37.1 years) and 20 controls (12 males, 8 females, mean age 36.1 years) both qualitatively and quantitatively using axial CT images and sagittal multi-planar reconstruction images of the lumbosacral region. For quantitative examination, we adopted two methods: method-1 (anteroposterior dural diameter of S1> L4) and method-2 (ratio of anteroposterior dural diameter/vertebral body diameter>cutoff values). The prevalence of dural ectasia among groups was compared by using Fisher's exact test and the Tukey–Kramer test.

Results: In LDS patients, the qualitative method showed 40% of dural ectasia, the quantitative method-1 50%, and the method-2 70%. In MFS patients, the corresponding prevalences were 50%, 75%, and 85%, and in controls, 0%, 0%, and 5%. Both LDS and MFS had a significantly wider dura than controls.

Conclusions: While the prevalence of dural ectasia varied depending on differences in qualitative and quantitative methods, LDS as well as MFS, showed, regardless of method, a higher prevalence of dural ectasia than controls. This finding should help the differentiation of LDS from controls.

Citation: Kono AK, Higashi M, Morisaki H, Morisaki T, Naito H, et al. (2013) Prevalence of Dural Ectasia in Loeys-Dietz Syndrome: Comparison with Marfan Syndrome and Normal Controls. PLoS ONE 8(9): e75264. doi:10.1371/journal.pone.0075264

Editor: Bart Dermaut, Pasteur Institute of Lille, France

Received April 17, 2013; **Accepted** August 12, 2013; **Published** September 25, 2013

Funding: Dr Hiroko Morisaki received a Health Labour Sciences Research Grant (Research on Measures for Intractable Diseases) from the Ministry of Health, Labour and Welfare. The funders had no role in study design, data collection and analysis, decision to publish, or preparation of the manuscript.

Competing Interests: The authors have declared that no competing interests exist.

* E-mail: akono@med.kobe-u.ac.jp

Introduction

Loeys–Dietz syndrome (LDS) is a newly discovered connective tissue disease caused by mutations in the gene of transforming growth factor β receptor (TGFBR) -1 or -2 [1,2]. The cardinal features of LDS consist of craniofacial features characterized by widely spaced eyes (orbital hypertelorism), bifid uvula and/or cleft palate, and cardiovascular diseases such as aortic root dilatation or aortic dissection, arterial tortuosity and aneurysms [2,3]. LDS shares many of its clinical features with Marfan syndrome (MFS) [4], which is an autosomal dominant connective tissue disorder caused by mutations in the gene of fibrillin-1 (FBN-1) [5]. The main features of MFS occur in skeletal, ocular, and cardiovascular areas, but other organs can also be affected, including skin, lung, and dura [6].

While LDS and MFS show striking pleiotropism and clinical variability, no clinical criteria for LDS have as yet been established in contrast to MFS, for which detailed diagnostic criteria have been developed [6,7]. The old 'Ghent nosology' for MFS classifies the clinical manifestations into major and minor criteria [6]. Dural ectasia (DE), which is also observed in neurofibromatosis type 1 and Ehlers–Danlos syndrome [6,8], is, after aortic dilatation/dissection, the second most common major criterion for MFS [8,9]. In the revised Ghent nosology, DE is no longer a critical criterion for MFS. As the finding of DE is used for the scoring of systemic features when the patients show aortic diseases, but do not have the ectopia lentis, the importance of DE remains in the new criteria. While the importance of DE is well recognized in MFS, only a few reports have dealt with the prevalence of DE in LDS [1,10,11]. DE usually occurs in connective tissues diseases, and occurs in the lumbar or sacral spine due to gravity. DE is characterized by widening of the spinal canal, posterior scalloping of the vertebral body, increased thinning of the cortex of pedicles and laminae, widening of the neural foramina or the presence of a meningocele [6]. While at present there is no standardized method for the diagnosis of DE, some qualitative [6,8] and quantitative methods [9,12,13] have been reported.

To establish clinical diagnostic criteria for LDS, the prevalence of DE has to be analyzed. In this study, we used qualitative and

quantitative methods to evaluate the prevalence of DE in LDS in comparison with that in MFS and controls.

Materials and Methods

The institutional review board (National Cardiovascular Research Center, Japan) approved this retrospective case-controlled study and written informed consent to analyze clinical data and gene mutations was obtained from all LDS and MFS subjects. In addition, written informed consent for the CT examinations was obtained from all subjects. The institutional review board waived written informed consent from the normal controls because this was a retrospective study.

Patient Population

The CT data in our institutional database was reviewed from June 2007 to July 2010. Ten LDS patients with an identified mutation in TGFBR (6 males, 4 females, mean age 36.3 years, range 20−54 years) were retrospectively reviewed from our institutional database which comprised about 20 LDS patients. These 10 patients had undergone CT examination in the lower abdominal and pelvic regions and were consecutively enrolled. Nine of them (90%) were in the post-operative stage (1 with aortic repair, 3 with valve replacement, and 5 with both). Reasons for hospitalization were aortic root dilatation in 4 patients and aortic dissection in 6 patients. Gene analysis showed 4 mutations in TGFBR-1 and 6 in TGFBR-2.

Twenty MFS patients with an identified mutation in FBN-1 (12 males, 8 females, mean age 37.1 years, range 20−56 years) were also reviewed. MFS patients who were matched to LDS patients in gender and age were randomly selected from our database, which comprises more than 100 MFS patients with mutation in FBN-1. Seventeen of the enrolled patients (85%) were in the post-operative stage (3 with aortic repair, 7 with valve replacement, and 7 with both). Reasons for hospitalization were aortic root dilatation in 11 patients, aortic dissection in 8 patients, and mitral valve regurgitation in 1 patient.

All LDS and MFS patients underwent clinical examinations including a physical examination and laboratory tests by a cardiovascular team. Initial and follow up CT examinations were performed in a clinical setting as described below. Genetic analysis was performed for all patients in the same manner as previously reported [11].

Twenty control subjects (12 males, 8 females, mean age 36.1 years, range 22−52 years) who were matched to LDS patients in gender and age were also randomly selected from our CT database. These subjects did not meet any of the major nor minor criteria of Ghent nosology. No gene analysis was performed for this group.

MFS patients and control subjects were matched to LDS in gender and age to avoid the need for adjusting the values of variables after they had been measured.

Imaging and Measurements

All LDS and MFS patients underwent CT examination (including CT angiography) using 16- or 64-MSCT at initial diagnosis or clinical follow-up for evaluation of the vascular tree. The CT covered the area from the thorax to the pelvis. Control subjects underwent CT examination covering the lower abdominal and pelvic regions as indicated by clinical need. Axial CT images with 2 mm slice thickness were obtained from all subjects and used to reconstruct multi-planar reconstruction (MPR) images. All images were transferred to CT image server and could be read on a PACS (Picture Archiving and Communication System) viewer. Two radiologists (A.K.K. and M.H. with 9 and 19 years experience, respectively, in diagnostic radiology) reviewed the CT images (qualitative inspection, described below) blinded to the genetic diagnosis. And one of the two radiologists (A.K.K.) evaluated CT images using the two quantitative methods described below.

Qualitative Inspection

DE is defined as widening of the spinal canal, posterior scalloping of the vertebral body, increased thinning of the cortex of pedicles and laminae, widening of the neural foramina or the presence of a meningocele [8,14,15]. The presence of an anterior sacral meningocele was diagnosed when herniation of the dural sac resulting from a defect in the anterior surface of the sacrum was seen [16]. Presence of a lateral meningocele was diagnosed when the nerve root sleeve was wide throughout the intervertebral foramen and ended in a pouch [17].

Quantitative Inspection

Method-1 proposed by Ahn et al. [9] (Fig. 1). Dural sac diameter (DSD) was measured in the mid-sagittal plane of the MPR image from the lumbus through to the sacrum. DE is diagnosed when the sagittal anteroposterior diameter of the spinal canal at S1 or below is greater than that at the mid axis of L4.

$$DE = DSD(S) > DSD(L4)$$

Method-2 proposed by Oosterhof et al. [12] (Fig. 1). The vertebral body diameter (VBD) and DSD were measured perpendicular to the long axis of the dural sac and vertebral body. VBD and DSD values were obtained at the midcorpus level of L1 to S1. The dural sac ratio (DSR) was calculated at L1 to S1 by dividing DSD by VBD. DE is considered present if DSR exceeds the cutoff value, which is defined as mean+2 SD of controls.

$$DSR = DSD/VBD$$

$$DE = DSR > \text{cutoff value at any level}$$

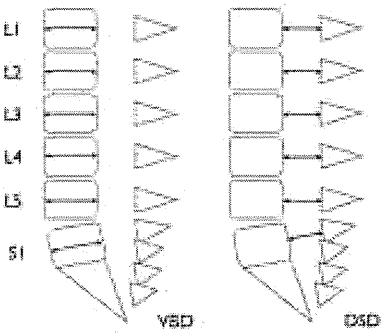

Figure 1. Scheme of sagittal CT images of the lumbosacral spine. Lines with arrows represent measurements of vertebral body diameters (VBD) and dural sac diameters (DSD).
doi:10.1371/journal.pone.0075264.g001

Statistical Analysis

For the statistical analysis, JMP software (version 8.0, SAS Institute Inc., CA, USA) was used. Continuous data were expressed as mean±SD.

We evaluated and compared the prevalence of DE in three groups by using one qualitative and two quantitative methods. The two-tailed student *t* test was used to compare continuous variables and Fisher's exact test for discrete variables. The DSRs among groups were evaluated with Tukey-Kramer test (alpha value of 0.05 was adopted). A p value <0.05 was considered statistically significant.

Results

Patient characteristics are listed in Table 1. There were no differences in sex and gender among the three groups.

The results obtained with the qualitative method (Table 1) showed that 4 (40%) LDS and 16 (80%) MFS patients possessed DE, but none of the control subject did. DE were thus more frequently observed in LDS and MFS than in control ($p = 0.0077$ and <0.001, respectively). There was no anterior meningocele in LDS or control, but one in MFS, while one lateral meningocele was observed in LDS (Fig. 2) and five in MFS, but none in control.

According to findings obtained with method-1 (Table 1), 5 (50%) LDS and 15 (75%) MFS patients possessed DE, and none of the control subjects did. Higher prevalence of DE in LDS and MFS than in control was also observed with this diagnostic method ($p = 0.0018$ and <0.0001, respectively).

According to findings obtained with method-2 (Table 1), LDS (at L2) and MFS (at L5, S1) patients had a higher prevalence of DE than control. Seven (70%) LDS and 17 (85%) MFS showed the presence of DE and one (5%) control also showed DE. Most MFS patients diagnosed with method-2 had DE at S1or L5 while few showed DE at other levels. In addition, LDS patients showed a diffusely wide dura from L1 through to S1 except for L4. The values for DSR are also listed in Table 2.

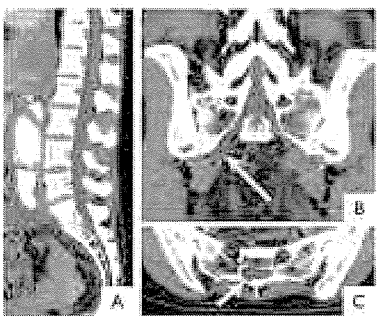

Figure 2. CT images of 46-year-old female with Loeys-Dietz syndrome. Sagittal image of the normal dura (A). Coronal image of right lateral meningocele (arrow) (B). Axial image at S1 shows asymmetric dilatation of the dura (arrow) (C). In this case, visual inspection could detect dural ectasia, but quantitative evaluation could not.
doi:10.1371/journal.pone.0075264.g002

Discussion

DE usually occurs in connective tissue diseases, and was one of the major diagnostic criteria for MFS [6]. DE is no longer a critical criterion for MFS; however, DE still is important because it is used in the scoring system in the revised version [7]. While the importance of DE is well recognized in MFS, its prevalence in LDS is unknown. Although there is at present no standardized diagnostic method for DE in LDS, some qualitative [6,8] and quantitative methods [9,12,13] have been used. In contrast to findings for MFS, only a few reports have dealt with the prevalence of DE in LDS [1,10,11]. Our study showed that LDS had a wider dural sac than control and the prevalence of DE in LDS was significantly higher than in control regardless of which

Table 1. Patient characteristics and prevalence of DE determined with qualitative and quantitative methods.

	LDS (n = 10)	MFS (n = 20)	Control (n = 20)	Difference*
Gene abnormality	TGFBR-1 or -2	FBN-1		
Gender (m:f)	6:4	12:8	12:8	NS
Age (y)	36.3±12.6	37.1±11.2	36.1±8.6	NS
No. of DE identified with qualitative method				
DE-positive	4 (40)	16 (80)	0 (0)	a, (p = 0.04); b, (p = 0.0077); c, (p<0.0001)
No. of DE identified with method-1				
DE-positive	5 (50)	15 (75)	0 (0)	b, (p = 0.0018); c, (p<0.0001)
No. of DE identified with method-2				
DE-positive at any level	7 (70)	17 (85)	1 (5)	b, (p = 0.00068); c, (p<0.0001)
L1	4 (40)	3 (15)	1 (5)	
L2	3 (30)	3 (15)	0 (0)	
L3	3 (30)	3 (15)	0 (0)	
L4	0 (0)	4 (20)	0 (0)	
L5	2 (20)	7 (35)	1 (5)	
S1	6 (60)	16 (80)	0 (0)	

LDS, Loeys-Dietz syndrome; MFS, Marfan syndrome; DSR, dural sac ratio; DE, dural ectasia; NS, not significant; a, difference between LDS and MFS; b, difference between LDS and control; c, difference between MFS and control.
Difference*, In this column, p values are shown. Differences were not tested for each level from L1 to S1.
doi:10.1371/journal.pone.0075264.t001

Table 2. Mean DSR values.

	LDS (n = 10)	MFS (n = 20)	Control (n = 20)	CI*
L1	0.56±0.08	0.52±0.12	0.48±0.06	NS
L2	0.53±0.09	0.49±0.12	0.45±0.06	b, 0.0004−0.17
L3	0.48±0.08	0.45±0.09	0.42±0.06	NS
L4	0.45±0.07	0.47±0.11	0.44±0.02	NS
L5	0.53±0.10	0.56±0.15	0.43±0.08	c, 0.04−0.22
S1	0.60±0.11	0.88±0.54	0.40±0.07	c, 0.21−0.74

DSR, dural sac ratio; LDS, Loeys-Dietz syndrome; MFS, Marfan syndrome; DE, dural ectasia; NS, not significant; a, difference between LDS and MFS; b, difference between LDS and control; c, difference between MFS and control. CI*, this column shows the confidence interval for significant differences.
doi:10.1371/journal.pone.0075264.t002

diagnostic method was used. According to the findings obtained with the methods used in our study, the prevalence of DE in LDS varied from 40 to 70%. This prevalence is higher than the 16% reported by Rodrigues et al. [10]. Although their report does not mention any details of diagnostic criteria for DE, they also used CT images. The reason for the difference between the two studies is not clear. In this study, DE was positive in 75–85% for MFS and 0–5% for NML. In a clinical setting, the differential diagnosis of LDS from MFS is problematic. Although the difference in DE frequency observed using a qualitative method is significant ($p = 0.04$) between LDS and MFS, the differences between method-1 and method-2 are not significant. This result shows that only knowing DE frequency would not be helpful when attempting to distinguish LDS from MFS. Further examination is needed to determine the differences that exist between these two genetic vascular disorders in addition to DE frequency.

Some reports about DE in MFS have emphasized quantitative methods because cutoff values can be used more uniformly than with qualitative methods [12,18]. However Lundby et al. reported that qualitative signs were very useful because 11.5% of their patients would not have been diagnosed with DE if lateral menigocele had not been adopted as a sign of DE [17]. Anterior and lateral meningocele has been identified as a strong qualitative indicator of DE in many studies [6,9,17]. We also propose the use of visual evaluation of DE, as presented in Fig. 2, because two (20%) LDS and three (6%) MFS patients were diagnosed by means of qualitative assessment although they were not diagnosed as such with method-1. As well as anterior or lateral meningocele, asymmetric dilatation such as scalloping of the vertebral body or widening of the neural foramina cannot be detected with qualitative evaluation in the mid-sagittal plain. In this study, the prevalence of anterior and lateral meningocele was lower than previously reported. This may be due to the lower contrast resolution of CT compared with MRI, which may lead to misdiagnosis of some meningoceles.

A higher prevalence of DSD at S1 than that at L4 (method-1) was used as a quantitative diagnostic method for DE [9] and resulted in assessment with high inter-observer agreement ($\kappa = 0.77$) [17]. This parameter can be easily and reliably measured in a routine clinical setting on CT and MRI, and previous studies have reported that it is also a useful marker for DE in [9,18]. Our result showed that five (50%) LDS and 15 (75%) MFS patients showed DE with this quantitative method in contrast to control (0%), which is consistent with previously reported findings. While this parameter is thus a useful diagnostic tool, it can be somewhat problematic in that the difference in DSD at L4 and S1 is often very small. There were a total of seven cases among the LDS and MFS patients in our study with differences of less than 2 mm. It is also problematic that diffuse ectasis throughout the lumbosacral regions is not detected with this method.

DSR (method-2), which Oosterhof et al. firstly described in 2001 [12], has been used to assess DE in recent studies [13,17]. The authors concluded that a combination of DSR above a given cutoff value at level L3 and S1 could be used to identify MFS with 95% sensitivity and 98% specificity. However, their method has been tested in later studies, but similar results have not been obtained [18,19]. Habermann et al. found a sensitivity of 56% and a specificity of 65% with an optimal cutoff value of 0.51 at S1 [18]. They suggested that some of the differences in cutoff values and accuracy were secondary to the age differences of the subjects enrolled in the two studies. Cutoff values depend on the characteristics of the control group such as age, ethnos, and diagnostic modality (i.e. CT or MRI). The main purpose of the cutoff values adopted for our study (means+2 SD of controls) was therefore to reduce the influence of such dependence. The DSRs reported by Lundby were 0.45, 0.43, 0.42, and 0.41 at L3, 4, 5, and S1, respectively [17], and those reported by Oosterhof were 0.48, 0.40, 0.35, 0.34, 0.32, and 0.35 at L1, 2, 3, 4, 5 and S1, respectively, [12]. These results were thus not so different from ours. By using our cutoff values, we identified DE in seven (70%) LDS and 17 (85%) MFS patients. Because most of LDS and MFS patients showed DE at S1, the prevalence of DE obtained with method-2 was equivalent to that obtained with method-1 in our study. As mentioned before, method-1 cannot identify an abnormality when the dilatation is diffuse (i.e., L4 was dilatated as well as S1). As seen in Table 2, LDS patients, in contrast to MFS patients, feature a diffuse dilatation, so that the use of cutoff values may help diagnose the dilatation of DE correctly even in LDS patients. In addition, the finding of the diffuse distribution of DE may help to identify LDS and distinguish it from MFS, although the difference between LDS and MFS was not significant in our study.

In a recent report, Soylen et al. reported 100% sensitivity and 94.7% specificity for a novel quantitative method using MRI images [13]. They adopted the value calculated by multiplying longitudinal diameter by wide diameter of the dura in axial plane for each level. They compared their results with those of Ahn and Oosterhof and found that sensitivity was equivalent for the three methods but their specificity was superior to Oosterhof's. We also adopted their qualitative method using CT images (unpublished data). While our results showed that many LDS and MFS patients had DE, the prevalence was very similar to that assessed with method-2. Soylen et al.'s method has a good diagnostic performance, but the measurements are rather time-consuming, so that the method proposed by Ahn or Oosterhof may be satisfactory for clinical settings.

Compared with CT, MRI is superior in quality of contrast resolution, especially in visualization of soft tissue. Therefore, most previous studies have used MRI imaging for the evaluation of DE [9,12,13]. However, thin slice data can now be obtained easily with CT, and MPR images derived form CT make it possible to analyze objects easily from any plane. In our institution, we usually reconstruct CT images of 2 mm slice thickness and diagnose them using a PACS viewer. Under these circumstances, we can reconstruct MPR images and analyze them within 5 min per patient. We applied MRI criteria for DE to our CT measurements. This is because we believed that these MRI criteria could be used with current CT images. As explained above, lateral and anterior meningocele constitutes an important finding of DE [17].

Reconstructed MPR CT images can also be used for the evaluation of both lateral and anterior meningocele. The fact that T2-weighted images on MRI are superior for detecting abnormalities with a water component makes the detection of lateral and anterior meningocele using MRI feasible. Moreover, careful reading of axial and MPR images of CT is sure to improve the detectability of anterior and lateral meningocele.

In this study, LDS showed a higher prevalence of DE than controls. If the presence of DE turns out to be a useful finding for differentiating LDS from controls, it may well become one of the diagnostic criteria. However, further study is needed to evaluate its diagnostic performance and feasibility.

Our study has certain limitations. First, while the number of patients in our study was very small, it is comparable with the numbers used in other studies. LDS patients in this study were consecutively recruited and represented the maximum number of this type of patient at that time. However, our study did not include patients aged <20 because there were no patients of that age in our hospital. This may have caused a patient selection bias, thereby influencing our results. Our results for MFS and controls were comparable with those of a study comprising a large number of MFS patients [17]. For LDS, on the other hand, further studies with a large number of subjects is necessary. Second, because to some extent DE develops with age, some patients may be without DE in spite of gene abnormalities. In this respect, we did not calculate either the sensitivity or specificity for the evaluation of the diagnostic performance against the genetic diagnosis as a reference standard. Of course, the prevalence of DE may fluctuate to some extent depending on the characteristics of the groups.

Conclusions

LDS as well as MFS showed a higher prevalence of DE than controls. The prevalence of DE in LDS varied from 40 to 70% depending on different qualitative and quantitative methods. These findings indicate that DE has the potential to become a diagnostic criterion for LDS.

Author Contributions

Conceived and designed the experiments: AKK HN KS. Performed the experiments: MH. Analyzed the data: AKK. Contributed reagents/materials/analysis tools: HM TM. Wrote the paper: AKK.

References

1. Loeys BL, Chen J, Neptune ER, Judge DP, Podowski M, et al. (2005) A syndrome of altered cardiovascular, craniofacial, neurocognitive and skeletal development caused by mutations in TGFBR1 or TGFBR2. Nat Genet 37: 275–281.
2. Loeys BL, Schwarze U, Holm T, Callewaert BL, Thomas GH, et al. (2006) Aneurysm syndromes caused by mutations in the TGF-beta receptor. N Engl J Med 355: 788–798.
3. Kono AK, Higashi M, Morisaki H, Morisaki T, Tsutsumi Y, et al. (2010) High prevalence of vertebral artery tortuosity of Loeys-Dietz syndrome in comparison with Marfan syndrome. Jpn J Radiol 28: 273–277.
4. Singh KK, Rommel K, Mishra A, Karck M, Haverich A, et al. (2006) TGFBR1 and TGFBR2 mutations in patients with features of Marfan syndrome and Loeys-Dietz syndrome. Hum Mutat 27: 770–777.
5. Dietz HC, Pyeritz RE, Hall BD, Cadle RG, Hamosh A, et al. (1991) The Marfan syndrome locus: confirmation of assignment to chromosome 15 and identification of tightly linked markers at 15q15-q21.3. Genomics 9: 355–361.
6. De Paepe A, Devereux RB, Dietz HC, Hennekam RC, Pyeritz RE (1996) Revised diagnostic criteria for the Marfan syndrome. Am J Med Genet 62: 417–426.
7. Loeys BL, Dietz HC, Braverman AC, Callewaert BL, De Backer J, et al. (2010) The revised Ghent nosology for the Marfan syndrome. J Med Genet 47: 476–485.
8. Fattori R, Nienaber CA, Descovich B, Ambrosetto P, Reggiani LB, et al. (1999) Importance of dural ectasia in phenotypic assessment of Marfan's syndrome. Lancet 354: 910–913.
9. Ahn NU, Sponseller PD, Ahn UM, Nallamshetty L, Rose PS, et al. (2000) Dural ectasia in the Marfan syndrome: MR and CT findings and criteria. Genet Med 2: 173–179.
10. Rodrigues VJ, Elsayed S, Loeys BL, Dietz HC, Yousem DM (2009) Neuroradiologic manifestations of Loeys-Dietz syndrome type 1. AJNR Am J Neuroradiol 30: 1614–1619.
11. Akutsu K, Morisaki H, Takeshita S, Sakamoto S, Tamori Y, et al. (2007) Phenotypic heterogeneity of Marfan-like connective tissue disorders associated with mutations in the transforming growth factor-beta receptor genes. Circ J 71: 1305–1309.
12. Oosterhof T, Groenink M, Hulsmans FJ, Mulder BJ, van der Wall EE, et al. (2001) Quantitative assessment of dural ectasia as a marker for Marfan syndrome. Radiology 220: 514–518.
13. Soylen B, Hinz K, Prokein J, Becker H, Schmidtke J, et al. (2009) Performance of a new quantitative method for assessing dural ectasia in patients with FBN1 mutations and clinical features of Marfan syndrome. Neuroradiology 51: 397–400.
14. De Paepe A (1999) Dural ectasia and the diagnosis of Marfan's syndrome. Lancet 354: 878–879.
15. Pyeritz RE, Fishman EK, Bernhardt BA, Siegelman SS (1988) Dural ectasia is a common feature of the Marfan syndrome. Am J Hum Genet 43: 726–732.
16. Oren M, Lorber B, Lee SH, Truex RC Jr, Gennaro AR (1977) Anterior sacral meningocele: report of five cases and review of the literature. Dis Colon Rectum 20: 492–505.
17. Lundby R, Rand-Hendriksen S, Hald JK, Lilleas FG, Pripp AH, et al. (2009) Dural ectasia in Marfan syndrome: a case control study. AJNR Am J Neuroradiol 30: 1534–1540.
18. Habermann CR, Weiss F, Schoder V, Cramer MC, Kemper J, et al. (2005) MR evaluation of dural ectasia in Marfan syndrome: reassessment of the established criteria in children, adolescents, and young adults. Radiology 234: 535–541.
19. Rose PS, Levy HP, Ahn NU, Sponseller PD, Magyari T, et al. (2000) A comparison of the Berlin and Ghent nosologies and the influence of dural ectasia in the diagnosis of Marfan syndrome. Genet Med 2: 278–282.

Surgical Experience With Aggressive Aortic Pathologic Process in Loeys-Dietz Syndrome

Yutaka Iba, MD, Kenji Minatoya, MD, Hitoshi Matsuda, MD, Hiroaki Sasaki, MD, Hiroshi Tanaka, MD, Hiroko Morisaki, MD, Takayuki Morisaki, MD, Junjiro Kobayashi, MD, and Hitoshi Ogino, MD

Departments of Cardiovascular Surgery and Bioscience and Genetics, National Cerebral and Cardiovascular Center, Osaka; Department of Cardiovascular Surgery, Tokyo Medical University, Tokyo, Japan

Background. Loeys-Dietz syndrome (LDS) is a recently recognized connective tissue disorder (CTD) caused by mutations in *transforming growth factor-beta receptor (TGFBR)1* and *TGFBR2*. Surgical outcomes of aortic repair in patients with LDS are poorly known.

Methods. We enrolled 16 patients with *TGFBR* mutations identified by gene analysis in this study. Between 1993 and 2011, they underwent 41 aortic surgical procedures. Ten patients (group D: dissection group) underwent aortic repair for acute or chronic aortic dissection as a first surgical intervention, and 6 patients (group N: nondissection group) underwent surgical treatment for aortic root dilatation. The mean follow-up period was 103.7 ± 92.3 months (range, 2– 276 months).

Results. There were no in-hospital deaths. In group N, valve-sparing root replacement (VSRR) was performed in all patients. The residual aorta in 9 patients (90%) from group D required further repairs, 3 times on average. Moreover, in 4 patients (40%), the aorta was entirely replaced in serial procedures. In group N, aortic dissection occurred in only 1 patient (17%). The aortic event-free rates at 5 years were 40% in group D and 80% in group N, respectively ($p = 0.819$). One late death due to arrhythmia occurred 1 month after VSRR. The cumulative survival rates at 5 years were 100% in group D and 83% in group N, respectively ($p = 0.197$).

Conclusions. Surgical outcomes for patients with LDS were satisfactory. Once aortic dissection occurred, the aorta expanded rapidly, requiring further operations. Therefore, early surgical intervention may improve prognosis by preventing a fatal aortic event.

(Ann Thorac Surg 2012;94:1413–7)

Loeys-Dietz syndrome (LDS) is a recently recognized connective tissue disorder (CTD) first described by Loeys and colleagues in 2005 [1] and resulting from mutations in *transforming growth factor-beta receptor (TGFBR)1* and *TGFBR2*. Phenotypic characteristics include arterial tortuosity, aortic aneurysms and dissections, ocular hypertelorism, bifid uvula, and cleft palate [1–3]. Of these characteristics, aortic lesions are considered to have the greatest influence on prognosis, similar to other CTDs such as Marfan's syndrome (MFS) or vascular-type Ehlers-Danlos syndrome. Indeed, some reports indicate that the aortic pathologic process in LDS is more aggressive and widespread than it is in MFS [2]. However surgical results and the postoperative prognosis of aortic repair in patients with LDS are not well known, although most patients require aortic operations.

In this study, we describe our surgical experience with aortic repair in patients with LDS with a severe aortic pathologic process.

Accepted for publication May 25, 2012.

Presented at the Poster Session of the Forty-eighth Annual Meeting of The Society of Thoracic Surgeons, Fort Lauderdale, FL, Jan 28–Feb 1, 2012.

Address correspondence to Dr Iba, 5-7-1 Fujishirodai, Suita, Osaka, 565-8565, Japan; e-mail: iba@hsp.ncvc.go.jp.

Patients and Methods

We performed genetic analysis in patients undergoing aortic surgical procedures at our center who were suspected of having a CTD because of young age, family history, typical annuloaortic ectasia (AAE), and so on. On the basis of the results, we enrolled 16 patients with mutations in *TGFBR1* or *TGFBR2* in this study (Table 1). Between 1990 and 2011, these patients collectively underwent 41 aortic operations. Mean age at the first operation was 31.4 ± 11.3 years. Nine patients had mutations in *TGFBR1* and 7 had mutations in *TGFBR2*. Ten patients underwent their first aortic operations after aortic dissection (group D: dissection group). In group D, indication for first surgical intervention was chronic type B aortic dissection in 6 patients and acute type A aortic dissection in 4 patients. Patients included a 20-year-old woman who at 19 weeks of pregnancy required urgent operation for acute type A aortic dissection. The first surgical intervention in the remaining 6 patients was for AAE without aortic dissection (group N: nondissection group).

Data were collected from hospital admission and outpatient medical records and telephone interviews. All patients were regularly assessed, either at our center or by a local cardiologist. The follow-up rate was 100%, and

Published by Elsevier Inc

0003-4975/$36.00
http://dx.doi.org/10.1016/j.athoracsur.2012.05.111

Abbreviations and Acronyms

AAE = annuloaortic ectasia
CSF = cerebrospinal fluid
CTD = connective tissue disorder
LDS = Loeys-Dietz syndrome
MFS = Marfan's syndrome
TGFBR = transforming growth factor-beta receptor
VSRR = valve-sparing root replacement

the mean follow-up period was 103.7 ± 92.3 months (range, 2–276 months). Our institution approved this retrospective study, and patient consent for our study was obtained either at the time of operation or when the patients came as outpatients.

Continuous variables were expressed as mean ± standard deviation and compared using the Student's *t* test. Categorical data were compared using Fisher's exact test. Survival and aortic event-free rates were estimated using the Kaplan-Meier method, and differences between each group were determined by log-rank analysis. *p* values of less than 0.05 were considered significant. Statistical analysis was performed using SPSS, version 17.0 for Windows (IBM SPSS Inc, Chicago, IL).

Results

No operative or in-hospital deaths occurred in our series. During postoperative hospitalization, there were 3 cerebrovascular events. Subdural hematoma occurred in 2 patients; 1 underwent descending thoracic aorta replacement and the other underwent thoracoabdominal aortic replacement for chronic type B aortic dissection. A third patient, who underwent emergency arch repair for acute type A aortic dissection, was diagnosed with cerebral infarction with right hemiparesis. The woman who needed emergency operation for acute aortic dissection during pregnancy safely gave birth to a baby 5 months after operation. In group N, valve-sparing root replacement (VSRR) was carried out in all 6 patients, and no major complications occurred in this group during hospitalization.

Follow-up results after the aortic procedures are shown in Table 2. Nine patients (90%) in group D required further aortic operations. Patients underwent a mean of 3 aortic procedures. Moreover, the aorta in 4 patients was entirely replaced through serial aortic operations. In group N, only 2 patients (33%) underwent further aortic repair. One patient underwent elective abdominal aortic replacement for an aneurysm of the abdominal aorta and bilateral common iliac artery, whereas another patient was diagnosed with acute dissection from the aortic arch to the terminal aorta 6 years after VSRR. After this, she needed a further aortic operation for dilatation of the dissected aorta. She finally achieved total aortic replacement 1 year after aortic dissection. The overall aortic event-free rates at 5 and 10 years were 46.4% and 18.6%, respectively (Fig 1). In the follow-up, there was only 1 late death resulting from arrhythmia. This patient, who was discharged uneventfully 12 days after VSRR for AAE, died suddenly 32 days after operation. The cumulative survival rate at 5 years was 93.8% in all patients (Fig 2).

Comment

Some phenotypic characteristics of LDS, such as aortic tortuosity and skeletal abnormality, overlap with those of MFS, a representative CTD, suggesting that to date LDS has been regarded as an MFS-like disease or practically treated as MFS. However important phenotypic differences have been described [1–4]. Characteristic craniofacial findings of LDS, such as hypertelorism, cleft palate, or bifid uvula, are seldom found in patients with MFS. In addition, some patients with LDS are not so tall, and lens dislocation, which is typical in MFS, is uncommon in patients with LDS.

Table 1. Patient Characteristics

Characteristic	Group D n = 10	Group N n = 6	*p* Value
Male sex	3	4	0.152
Mean age at first operation	36.0 ± 12.2	23.7 ± 5.4	0.357
Genetic mutation			
TGFBR 1	6	3	0.696
TGFBR 2	4	3	
Mean number of aortic operations	3.0 ± 1.2	1.8 ± 1.5	0.125
Type of aortic operation			
Root replacement			
VSRR	3[a]	6	
Bentall	7[a]	0	
Arch repair	7	1	
DTAA repair	5	1	
TAAA repair	5	1	
AAA repair (infrarenal)	3	2	
Preoperative AI before VSRR			
None	0	1	
Trivial	1	2	
Mild	2	2	
Moderate	0	1	
Severe	0	0	
Postoperative AI after VSRR			
None	1	4	
Trivial	2	2	
Mild	0	0	
Moderate	0	0	
Severe	0	0	

[a] Including concomitant arch repair.

AAA = abdominal aortic aneurysm; AI = aortic insufficiency; DTAA = descending thoracic aortic aneurysm; TAAA = thoracoabdominal aortic aneurysm; *TGFBR = transforming growth factor beta receptor*; VSRR = valve-sparing root replacement.